

Mathematical Models of Contemporary Elementary Quantum Computing Devices

G. Chen, D. A. Church, B.-G. Englert, and M. S. Zubairy

ABSTRACT. Computations with a future quantum computer will be implemented through the operations by elementary quantum gates. It is now well known that the collection of 1-bit and 2-bit quantum gates are universal for quantum computation, i.e., any n -bit unitary operation can be carried out by concatenations of 1-bit and 2-bit elementary quantum gates.

Three contemporary quantum devices—cavity QED, ion traps and quantum dots—have been widely regarded as perhaps the most promising candidates for the construction of elementary quantum gates. In this paper, we describe the physical properties of these devices, and show the mathematical derivations based on the interaction of the laser field as control with atoms, ions or electron spins, leading to the following:

- (i) the 1-bit unitary rotation gates; and
- (ii) the 2-bit quantum phase gates and the controlled-not gate.

This paper is aimed at providing a sufficiently self-contained survey account of analytical nature for mathematicians, physicists and computer scientists to aid interdisciplinary understanding in the research of quantum computation.

1. Introduction

The design and construction of the quantum computer is a major project by the scientific community of the 21st Century. This project is interdisciplinary by nature, requiring close collaboration between physicists, engineers, computer scientists and mathematicians.

Physicists have taken the lead in the design of quantum devices utilizing the peculiar properties of quantum mechanics. Most or perhaps all of such devices will eventually become micro- or nano-fabricated. Their controls are achieved through the tuning of laser pulses. As hardware, many types of material or devices have been either used or proposed: NMR, cavity QED, ion or atom traps, quantum dots, SQUID, etc. See some discussions in [20, Chap. 7], [27], for example. NMR (nuclear magnetic resonance) is the first scheme utilized by researchers to demonstrate the principle of quantum computing through quantum search. NMR seems to have

The first and fourth authors are also of the Institute of Quantum Studies, Texas A&M University, College Station, TX 77843, U.S.A., and are supported in part by DARPA QuIST Contract F49620-01-1-0566 and Texas A&M University TITF initiative. The third author was supported in part by NSF Grant PHY9876899.

provided the most successful demonstration of quantum computing so far. However, this kind of “quantum computing in a coffee mug” utilizes bulk material, which is not considered as really quantum by many people. In addition, NMR has a severe weakness in the lack of scalability. Concerning SQUIDs¹ (superconducting quantum interference devices), there has been major progress in the design and control of such devices recently. However, the authors’ analytical knowledge about SQUIDs still appears very limited for the time being and, thus, any detailed mathematical representations must be deferred to a future account.

We focus our attention on the following three quantum devices: cavity QED, ion traps and quantum dots. They seem to have received the most attention in the contemporary literature, and have been widely identified by many as the most promising. The writing of this paper all began with our simple desire to try to understand, analytically, how and why such devices work. Analytical studies of these devices are scattered in many references in the physics literature, which admittedly are not easy reading for most mathematicians. Indeed, this is the most commonly encountered difficulty in any interdisciplinary research. But even many physicists specializing in quantum devices find certain difficulty in their attempt to understand the working of other quantum devices, if such devices do not fall exactly within their own specialty. Therefore, our objectives in this paper are three-fold:

- (1) Provide a sufficiently self-contained account of the physical description of these primary contemporary quantum computing devices and the derivation of their mathematical representations.
- (2) Supply the control-theoretic aspect of quantum control via the shaping of laser pulses in quantum computing, which is the main theme of the conference.
- (3) Write an accessible survey of three important quantum devices for mathematicians and other scientists who are interested in understanding the basic interdisciplinary link between physics, mathematics and computer science, in a mathematically rigorous way, for quantum computing.

Our main emphasis will be on the mathematical modeling. As far as the physics is concerned in this paper, we acknowledge the many segments that we have extracted, directly or indirectly, from the original sources cited in the references. New devices and designs emerge almost daily, and we must concede that the list of references is neither exhaustively comprehensive nor totally up-to-date as any attempt to achieve such by us is nearly impractical, or even impossible given the time and various other constraints. We nevertheless believe that the basic mathematics underlying most of the quantum computing devices remains largely similar, and hope that we have provided enough ideas and information for the readers to trace the literature on their own.

¹The SQUID can be viewed as a high- Q microwave frequency LC resonator. The first excited state, with excitation energy $\hbar\omega$ where ω is the microwave frequency, is doubly degenerate in zero magnetic field. These two states are the qubit states. To lift the degeneracy, Josephson junction(s) are placed in the current loop. Magnetic field can then be used to tune the levels back to degeneracy as required for qubit coupling, etc. The coupling is magnetic, as in mutual inductance of two current loops.

The major breakthrough made last year (2001–02) is the single quantum flux gate for readout. It is 100% efficient and does not add decoherence. Expect to see rapid progress in the near future as a result of this breakthrough.

We thank Prof. Philip R. Hemmer for the above communication.

In the main body of this paper to follow, there are four sections. Section 2 provides a quick summary of universality results of quantum gates. Sections 3, 4 and 5 deal with, respectively, cavity QED, ion traps and quantum dots. In the final Section 6, we briefly discuss some issues on laser control in quantum computing as the conclusion of this paper.

2. Universality of Elementary Quantum Gates

We begin this section by introducing some basic notations used in quantum mechanics, as such notations do not appear to be familiar to a majority of mathematicians. A useful reference can be found in [25].

Let \mathcal{H} be a *complex* Hilbert space with inner product $\langle \cdot, \cdot \rangle$. For any subset $S \subseteq \mathcal{H}$, define

$$(2.1) \quad \text{span } S = \text{closure of } \left\{ \sum_{j=1}^n \alpha_j \psi_j \mid \alpha_j \in \mathbb{C}, \psi_j \in S, j = 1, 2, \dots, n, \text{ for all } \psi_j \in S \right\} \text{ in } \mathcal{H},$$

where in the above, \mathbb{C} denotes the set of all complex numbers. Elements in \mathcal{H} , such as ψ_j in (2.1), are called vectors. The inner product of two vectors ψ_j and ψ_k is $\langle \psi_j, \psi_k \rangle$. However, in quantum mechanics, the Dirac bra-ket notation writes the vector ψ_k as $|k\rangle$, pronounced *ket k*, where k labels the vector. The role of ψ_j in the inner product $\langle \psi_j, \psi_k \rangle$ is that ψ_j is identified as a linear functional on \mathcal{H} by

$$(2.2) \quad \psi_j^*: \mathcal{H} \longrightarrow \mathbb{C}; \quad \psi_j^*(\psi_k) \equiv \langle \psi_j, \psi_k \rangle.$$

The Dirac bra-ket notation writes ψ_j^* as $\langle j|$, pronounced *bra j*. The inner product is now written as

$$(2.3) \quad \langle \psi_j, \psi_k \rangle = \langle j|k \rangle.$$

Let $A: \mathcal{H} \rightarrow \mathcal{H}$ be a linear operator. Then in Dirac's notation we write $\langle \psi_j, A\psi_k \rangle$ as $\langle j|A|k \rangle$.

The set of all kets ($|k\rangle$) generates the linear space \mathcal{H} , and the set of all bras ($\langle j|$) also generates the dual linear space \mathcal{H}^* . These two linear spaces are called, respectively, the ket space and the bra space, which are dual to each other. The natural isomorphism from H onto H^* , or from H^* onto H , is called “taking the adjoint” by physicists. An expression like $\langle j|A|k \rangle$ has an intended symmetry: one can think of A acting on $|k\rangle$ on the right as a matrix times a column vector, or A acting on $\langle j|$ on the left as a row vector times a matrix.

Any 2-dimensional complex Hilbert space \mathcal{H} is isomorphic to \mathbb{C}^2 . The standard basis of \mathbb{C}^2 is

$$(2.4) \quad \mathbf{e}_1 = \begin{bmatrix} 1 \\ 0 \end{bmatrix}, \quad \mathbf{e}_2 = \begin{bmatrix} 0 \\ 1 \end{bmatrix}.$$

In quantum mechanics, the preferred notation for basis is, respectively, $|0\rangle$ and $|1\rangle$, where $|0\rangle$ and $|1\rangle$ generally refer to the “spin” state of a certain quantum system under discussion. “Spin up” and “spin down” form a binary quantum alternative and, therefore, a quantum bit or, a *qubit*. These spin states may then further be identified with \mathbf{e}_1 and \mathbf{e}_2 through, e.g.,

$$(2.5) \quad |0\rangle = \begin{bmatrix} 1 \\ 0 \end{bmatrix}, \quad |1\rangle = \begin{bmatrix} 0 \\ 1 \end{bmatrix}.$$

For a column vector, say \mathbf{e}_1 , we use superscript T to denote its transpose, such as $\mathbf{e}_1^T = [1 \ 0]$, for example. The spin states $|0\rangle$ and $|1\rangle$ form a standard orthonormal basis for the (single) qubit's ket space. The tensor product of a set of n vectors $|z_j\rangle \in \mathbb{C}_j^2$, specified by the quantum numbers z_j for $j = 1, 2, \dots, n$, is written interchangeably as

$$(2.6) \quad |z_1\rangle \otimes |z_2\rangle \otimes \cdots \otimes |z_n\rangle = |z_1\rangle |z_2\rangle \cdots |z_n\rangle = |z_1 z_2 \cdots z_n\rangle.$$

The tensor product space of n copies of \mathbb{C}_2 is defined to be

$$(2.7) \quad (\mathbb{C}_2)^{\otimes n} = \text{span}\{|j_1 j_2 \cdots j_n\rangle \mid j_k \in \{0, 1\}, k = 1, 2, \dots, n\}.$$

It is a 2^n -dimensional complex Hilbert space with the induced inner product from \mathbb{C}^2 . A *quantum state* is a vector in $(\mathbb{C}^2)^{\otimes n}$ (or in any Hilbert space \mathcal{H}) with the unit norm². A quantum state is said to be *entangled* if it is *not* a tensor product of the form (2.6). A *quantum operation* is a *unitary linear transformation* on \mathcal{H} . The *unitary group* $U(\mathcal{H})$ on \mathcal{H} consists of all unitary linear transformations on \mathcal{H} with composition as the (noncommutative) natural multiplication operation of the group.

It is often useful to write the basis vectors $|j_1 j_2 \cdots j_n\rangle \in (\mathbb{C}^2)^{\otimes n}$, $j_k \in \{0, 1\}$, $k = 1, 2, \dots, n$, as column vectors according to the lexicographic ordering:

$$(2.8) \quad \begin{aligned} |00 \cdots 00\rangle &= \begin{bmatrix} 1 \\ 0 \\ 0 \\ \vdots \\ 0 \\ 0 \\ 0 \\ 0 \end{bmatrix}, |00 \cdots 01\rangle = \begin{bmatrix} 0 \\ 1 \\ 0 \\ \vdots \\ 0 \\ 0 \\ 0 \\ 0 \end{bmatrix}, |00 \cdots 10\rangle = \begin{bmatrix} 0 \\ 0 \\ 1 \\ \vdots \\ 0 \\ 0 \\ 0 \\ 0 \end{bmatrix}, \dots \\ |11 \cdots 10\rangle &= \begin{bmatrix} 0 \\ 0 \\ 0 \\ \vdots \\ 0 \\ 1 \\ 1 \\ 0 \end{bmatrix}, |11 \cdots 11\rangle = \begin{bmatrix} 0 \\ 0 \\ 0 \\ \vdots \\ 0 \\ 0 \\ 1 \\ 1 \end{bmatrix}; \end{aligned}$$

cf. (2.5). Any 2×2 unitary matrix is an admissible quantum operation on one qubit. We call it a 1-bit gate. Similarly, we call a $2^k \times 2^k$ unitary transformation a k -bit gate. Let a 1-bit gate be

$$(2.9) \quad U = \begin{bmatrix} u_{00} & u_{01} \\ u_{10} & u_{11} \end{bmatrix};$$

we define the operator $\Lambda_m(U)$ [3] on $(m+1)$ -qubits (with $m = 0, 1, 2, \dots$) through its action on the basis by

$$(2.10) \quad \Lambda_m(U)(|x_1 x_2 \cdots x_m y\rangle) = \begin{cases} |x_1 x_2 \cdots x_m y\rangle & \text{if } \bigwedge_{k=1}^m x_k = 0, \\ u_{0y}|x_1 x_2 \cdots x_m 0\rangle + u_{1y}|x_1 x_2 \cdots x_m 1\rangle & \text{if } \bigwedge_{k=1}^m x_k = 1, \end{cases}$$

²This type of quantum state is actually a more restrictive type, called a *pure state*. A pure state, say ket $|k\rangle$, could be identified with the projection operator $|k\rangle\langle k|$. Then a *general state* is a convex sum of such projectors, i.e., $\sum_k c_k |k\rangle\langle k|$ with $c_k \geq 0$ and $\sum_k c_k = 1$.

where “ \wedge ” denotes the Boolean operator AND. The matrix representation for $\Lambda_m(U)$ according to the ordered basis (2.8) is

$$(2.11) \quad \Lambda_m(U) = \begin{bmatrix} 1 & & & & \\ & \ddots & & & \\ & & 1 & & \bigcirc \\ & & & \bigcirc & \\ & \bigcirc & & \begin{bmatrix} u_{00} & u_{01} \\ u_{10} & u_{11} \end{bmatrix} & \end{bmatrix}_{2^{m+1} \times 2^{m+1}}.$$

This unitary operator is called the m -bit-controlled U operation.

An important logic operation on one qubit is the NOT-gate

$$(2.12) \quad \sigma_x = \begin{bmatrix} 0 & 1 \\ 1 & 0 \end{bmatrix};$$

cf. the Pauli matrices in (5.2) of Section 5. From σ_x , define the important 2-bit operation $\Lambda_1(\sigma_x)$, which is the controlled-not gate, henceforth acronymed the CNOT gate.

For any 1-bit gate A , denote by $A(j)$ the operation (defined through its action on the basis) on the slot j :

$$(2.13) \quad A(j)|x_1 x_2 \cdots x_j \cdots x_n\rangle = |x_1\rangle \otimes |x_2\rangle \otimes \cdots \otimes |x_{j-1}\rangle \otimes [A|x_j\rangle] \otimes |x_{j+1}\rangle \otimes \cdots \otimes |x_n\rangle.$$

Similarly, for a 2-bit gate B , we define $B(j, k)$ to be the operation on the two qubit slots j and k [4]. A simple 2-bit gate is the swapping gate

$$(2.14) \quad U_{\text{sw}}|x_1 x_2\rangle = |x_2 x_1\rangle, \text{ for } x_1, x_2 \in \{0, 1\}.$$

Then $U_{\text{sw}}(j, k)$ swaps the qubits between the j -th and the k -th slots.

The tensor product of two 1-bit quantum gates S and T is defined through

$$(2.15) \quad (S \otimes T)(|x\rangle \otimes |y\rangle) = (S|x\rangle) \otimes (T|y\rangle), \text{ for } x, y \in \{0, 1\}.$$

A 2-bit quantum gate V is said to be *primitive* ([4, Theorem 4.2]) if

$$(2.16) \quad V = S \otimes T \quad \text{or} \quad V = (S \otimes T)U_{\text{sw}}$$

for some 1-bit gates S and T . Otherwise, V is said to be *imprimitive*.

It is possible to factor an n -bit quantum gate U as the composition of k -bit quantum gates for $k \leq n$. The earliest result of this *universality* study was given by Deutsch [8] in 1989 for $k = 3$. Then in 1995, Barenco [2], Deutsch, Barenco and Ekert [9], DiVincenzo [12] and Lloyd [16] gave the result for $k = 2$. Here, we quote the elegant mathematical treatment and results by J.-L. Brylinski and R. K. Brylinski in [4].

DEFINITION 2.1 ([4, Def. 4.2]). A collection of 1-bit gates A_i and 2-bit gates B_j is called (exactly) *universal* if, for each $n \geq 2$, any n -bit gate can be obtained by composition of the gates $A_i(\ell)$ and $B_j(\ell, m)$, for $1 \leq \ell, m \leq n$. \square

THEOREM 2.1 ([4, Theorem 4.1]). *Let V be a given 2-bit gate. Then the following are equivalent:*

- (i) *The collection of all 1-bit gates A together with V is universal.*
- (ii) *V is imprimitive.* \square

A common type of 1-bit gate from AMO (atomic, molecular and optical) devices is the unitary rotation gate

$$(2.17) \quad U_{\theta,\phi} \equiv \begin{bmatrix} \cos \theta & -ie^{-i\phi} \sin \theta \\ -ie^{i\phi} \sin \theta & \cos \theta \end{bmatrix}, \quad 0 \leq \theta, \phi \leq 2\pi.$$

We have (the determinant) $\det U_{\theta,\phi} = 1$ for any θ and ϕ and, thus, the collection of all such $U_{\theta,\phi}$ is not dense in $U(\mathbb{C}^2)$. Any unitary matrix with determinant equal to 1 is said to be *special unitary* and the collection of all special unitary matrices on $(\mathbb{C}^2)^{\otimes n}$, $SU((\mathbb{C}^2)^{\otimes n})$, is a proper subgroup of $U((\mathbb{C}^2)^{\otimes n})$. It is known that the gates $U_{\theta,\phi}$ generate $SU(\mathbb{C}^2)$.

Another common type of 2-bit gate we shall encounter in the next two sections is the quantum phase gate (QPG)

$$(2.18) \quad Q_\eta = \begin{bmatrix} 1 & 0 & 0 & 0 \\ 0 & 1 & 0 & 0 \\ 0 & 0 & 1 & 0 \\ 0 & 0 & 0 & e^{i\eta} \end{bmatrix}, \quad 0 \leq \eta \leq 2\pi.$$

THEOREM 2.2 ([4, Theorem 4.4]). *The collection of all the 1-bit gates $U_{\theta,\phi}$, $0 \leq \theta, \phi, \phi \leq 2\pi$, together with any 2-bit gate Q_η where $\eta \not\equiv 0 \pmod{2\pi}$, is universal.* \square

Note that the CNOT gate $\Lambda_1(\sigma_x)$ can be written as

$$(2.19) \quad \Lambda_1(\sigma_x) = U_{\pi/4, \pi/2}(2) Q_\pi U_{\pi/4, -\pi/2}(2);$$

cf. [10, (2.2)]. Thus, we also have the following.

COROLLARY 2.3. *The collection of all the 1-bit gates $U_{\theta,\phi}$, $0 \leq \theta, \phi \leq 2\pi$, together with the CNOT gate $\Lambda_1(\sigma_x)$, is universal.* \square

Diagrammatically, the quantum circuit for (2.19) is given in Fig. 2.1.

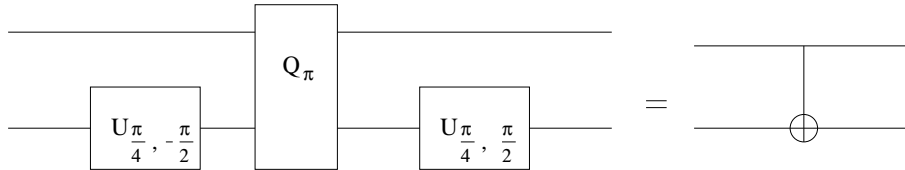


FIGURE 2.1. The quantum circuits for equation (2.19). The top wire represents the leading qubit (which is the most significant), while the second wire represents the second qubit.

3. Two-Level Atoms and Cavity QED

The main objective of this section is to show that the 1-bit unitary gates (2.17) and the 2-bit QPG (2.18) can be implemented using the methods of, respectively, 2-level atoms and cavity QED. For clarity, we divide the discussions in three sub-sections.

3.1. Two-Level Atoms. The atomic energy levels are very susceptible to excitation by electromagnetic radiation. The structure of electronic eigenstates and the interaction between electrons and photons can be quite complicated. But under certain assumptions we have in effect a 2-level atom. These assumptions are as follows:

- (i) the difference in energy levels of the electrons matches the energy of the incident photon;
- (ii) the symmetries of the atomic structure and the resulting “selection rules” allow the transition of the electrons between the two levels; and
- (iii) all the other levels are sufficiently “detuned” in frequency separation with respect to the frequency of the incident field such that there is no transition to those levels.

Then the model of a 2-level atom provides a good approximation.

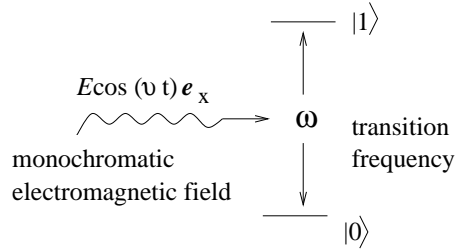


FIGURE 3.1. A 2-level atom, where a bound electron in an atom interacts with an external electromagnetic field.

The wave function $\psi(\mathbf{r}, t)$ of the electron of the 2-level atom, which is coupled to the external electric field $\mathbf{E}(\mathbf{r}, t)$ by its electric charge e , as shown in Fig. 3.1, obeys the Schrödinger equation

$$(3.1) \quad i\hbar \frac{\partial}{\partial t} \psi(\mathbf{r}, t) = H \psi(\mathbf{r}, t) = (H_0 + H_1) \psi(\mathbf{r}, t),$$

where $|\psi(\mathbf{r}, t)|^2$ is the probability density of finding that electron at position $\mathbf{r} = (x, y, z)$ at time t , and

$$(3.2) \quad H_0 \equiv \frac{1}{2m} \nabla^2 + V(\mathbf{r})$$

is the differential operator for the unperturbed Hamiltonian of the electron, with the gradient operator $\nabla = (\partial/\partial x, \partial/\partial y, \partial/\partial z)$ and the electrostatic potential $V(\mathbf{r})$ between the electron and the nucleus,

$$(3.3) \quad H_1 \equiv -e\mathbf{r} \cdot \mathbf{E}(\mathbf{r}_0, t)$$

is the interaction Hamiltonian between the field and the electron of the atom.

REMARK 3.1. The wavelength of visible light, typical for atomic transitions, is about a few thousand times the diameter of an atom. Therefore, there is no significant spatial variation of the electric field across an atom and so we can replace $\mathbf{E}(\mathbf{r}, t)$ by $\mathbf{E}(\mathbf{r}_0, t)$, the field at a reference point inside the atom such as the position of the nucleus or the center of mass. Consistent with this long-wavelength approximation (known as *dipole approximation* in the physics literature) is that the magnetic field \mathbf{B} satisfies $\mathbf{B}(\mathbf{r}, t) \cong 0$, so that the Lorentz force of the radiation field

on the electron is $e\mathbf{E}(\mathbf{r}_0, t)$, the negative gradient of $-e\mathbf{r} \cdot \mathbf{E}(\mathbf{r}_0, t)$, which adds to the potential energy $V(\mathbf{r})$ in the Hamiltonian operator. \square

Let the external electromagnetic field be a monochromatic plane-wave field linearly polarized along the x -axis, which interacts with the atom placed at $\mathbf{r}_0 = \mathbf{0}$. The electric field takes the form

$$(3.4) \quad \mathbf{E}(\mathbf{0}, t) = \mathcal{E} \cos(\nu t) \mathbf{e}_x; \quad \mathbf{e}_x \equiv [1, 0, 0]^T.$$

Let $|1\rangle$ and $|0\rangle$ represent upper and lower level states of the atom, which are eigenstates of the unperturbed part H_0 of the Hamiltonian corresponding to the eigenvalues $\hbar\omega_1$ and $\hbar\omega_0$, respectively, with $\omega \equiv \omega_1 - \omega_0$, cf. Fig. 3.1.

For the unperturbed 2-level atom system, i.e., without the external electromagnetic field, let the eigenstates of the electron be $|\psi_0\rangle = |0\rangle$ and $|\psi_1\rangle = |1\rangle$, i.e.,

$$(3.5) \quad \begin{cases} H_0|\psi_0\rangle = E_0|\psi_0\rangle, & \text{or } H_0|0\rangle = \hbar\omega_0|0\rangle; & \langle 0|0\rangle = 1, \\ H_0|\psi_1\rangle = E_1|\psi_1\rangle, & \text{or } H_0|1\rangle = \hbar\omega_1|1\rangle; & \langle 1|1\rangle = 1. \end{cases}$$

We invoke the assumption of 2-level atom that the electron lives only on states $|0\rangle$ and $|1\rangle$:

$$(3.6) \quad |\psi(t)\rangle = C_0(t)|0\rangle + C_1(t)|1\rangle,$$

where $C_0(t)$ and $C_1(t)$ are complex-valued functions such that $|C_0(t)|^2 + |C_1(t)|^2 = 1$, with $|C_0(t)|^2$ and $|C_1(t)|^2$ being the probability of the electron in, respectively, state $|0\rangle$ and $|1\rangle$ at time t .

Since H_1 (after quantization) is an operator effective only on the subspace

$$(3.7) \quad S = \text{span}\{|0\rangle, |1\rangle\},$$

H_1 is the zero operator on S^\perp (the orthogonal complement of S in the Hilbert space \mathcal{H} which has an orthonormal basis consisting of all eigenstates of H_0). We utilize the property that on S the projection operator is $|0\rangle\langle 0| + |1\rangle\langle 1|$, and obtain

$$(3.8) \quad \begin{aligned} H_1 &= -e\mathbf{r} \cdot \mathbf{E}(\mathbf{0}, t) = -e(x\mathbf{e}_x + y\mathbf{e}_y + z\mathbf{e}_z) \cdot (\mathcal{E} \cos(\nu t) \mathbf{e}_x) \\ &= -e\mathcal{E}x \cos(\nu t) \quad (\text{by (3.3) and (3.4)}) \\ &= -e\mathcal{E}[|0\rangle\langle 0| + |1\rangle\langle 1|]x[|0\rangle\langle 0| + |1\rangle\langle 1|] \cos(\nu t) \\ &= -e\mathcal{E}\{[\langle 0|x|0\rangle]|0\rangle\langle 0| + [\langle 0|x|1\rangle]|0\rangle\langle 1| \\ &\quad + [\langle 1|x|0\rangle]|1\rangle\langle 0| + [\langle 1|x|1\rangle]|1\rangle\langle 1|\} \cos(\nu t). \end{aligned}$$

But from the symmetry property and the selection rules that $|\psi_j(\mathbf{r})|^2 = |\psi_j(-\mathbf{r})|^2$ for $j = 0$ and 1 , we have

$$(3.9) \quad \langle 0|x|0\rangle = \int_{-\infty}^{\infty} \int_{-\infty}^{\infty} \int_{-\infty}^{\infty} x |\psi_0(\mathbf{r})|^2 dx dy dz = 0$$

since $x = \mathbf{r} \cdot \mathbf{e}_x$ is an odd function of \mathbf{r} whereas $|\psi_0(\mathbf{r})|^2$ is even. Similarly, $\langle 1|x|1\rangle = 0$. Now, write $P_{01} \equiv e\langle 0|x|1\rangle$ and $P_{10} \equiv e\langle 1|x|0\rangle$. Then $P_{10} = \overline{P_{01}}$. To solve the partial differential equation (3.1), we need only focus our attention on the 2-dimensional invariant subspace S and, thus, a dramatic reduction of dimensionality.

Substituting (3.6) into (3.1), utilizing (3.5) and (3.8) and simplifying, we obtain a 2×2 first order linear ODE

$$(3.10) \quad \frac{d}{dt} \begin{bmatrix} C_0(t) \\ C_1(t) \end{bmatrix} = \begin{bmatrix} -i\omega_0 & i\Omega_R e^{-i\phi} \cos \nu t \\ i\Omega_R e^{i\phi} \cos \nu t & -i\omega_1 \end{bmatrix} \begin{bmatrix} C_0(t) \\ C_1(t) \end{bmatrix},$$

where

$$(3.11) \quad \Omega_R \equiv \frac{|P_{10}|\mathcal{E}}{\hbar} = \text{the Rabi frequency},$$

and

$$(3.12) \quad \phi = \text{phase of } P_{10}: P_{10} = |P_{10}|e^{i\phi}.$$

Equation (3.10) has time-varying coefficients and exact solutions of such equations are not always easy to come by. Here, we make another round of approximation, called the *rotating wave approximation*, by first setting

$$(3.13) \quad c_0(t) = C_0(t)e^{i\omega_0 t}, \quad c_1(t) = C_1(t)e^{i\omega_1 t},$$

and substituting them into (3.10) and then dropping terms involving $e^{\pm i(\omega+\nu)t}$, where $\omega \equiv \omega_0 - \omega_1$ is called the atomic transition frequency. (From an experimental point of view, such $e^{\pm i(\omega+\nu)t}$ terms represent high frequency oscillations which cannot be observed in laboratory instrumentation. Furthermore, integrals involving highly oscillatory terms make insignificant contributions. In view of the fact that other non-resonant terms have already been discarded, these $e^{\pm i(\omega+\nu)t}$ terms representing highly non-resonant contributions should be neglected for consistency.) Then we obtain

$$(3.14) \quad \begin{cases} \dot{c}_0(t) = \frac{i\Omega_R}{2} e^{-i\phi} e^{i(\omega-\nu)t} c_1(t), \\ \dot{c}_1(t) = \frac{i\Omega_R}{2} e^{i\phi} e^{-i(\omega-\nu)t} c_0(t), \end{cases}$$

which in turn leads to a second order single ODE with constant coefficients

$$(3.15) \quad \ddot{c}_0 - i(\omega - \nu)\dot{c}_0 + \frac{\Omega_R^2}{4}c_0 = 0.$$

Solving for c_0 and c_1 in (3.14) and (3.15), we obtain the explicit solution in terms of the initial condition $(c_0(0), c_1(0))$:

$$(3.16) \quad \begin{bmatrix} c_0(t) \\ c_1(t) \end{bmatrix} = \begin{bmatrix} e^{i\frac{\Delta}{2}t} \left[\cos\left(\frac{\Omega}{2}t\right) - i\frac{\Delta}{\Omega} \sin\left(\frac{\Omega}{2}t\right) \right] & e^{i\frac{\Delta}{2}t} \cdot i \cdot \frac{\Omega_R}{\Omega} e^{-i\phi} \sin\left(\frac{\Omega}{2}t\right) \\ e^{-i\frac{\Delta}{2}t} \cdot i \frac{\Omega_R}{\Omega} e^{i\phi} \sin\left(\frac{\Omega}{2}t\right) & e^{-i\frac{\Delta}{2}t} \left[\cos\left(\frac{\Omega}{2}t\right) + i\frac{\Delta}{\Omega} \sin\left(\frac{\Omega}{2}t\right) \right] \end{bmatrix} \begin{bmatrix} c_0(0) \\ c_1(0) \end{bmatrix},$$

where $\Omega = \sqrt{\Omega_R^2 + (\omega - \nu)^2}$. At resonance,

$$(3.17) \quad \Delta = \omega - \nu = 0,$$

and, thus

$$(3.18) \quad \frac{\Delta}{\Omega} = 0, \quad \Omega_R = \Omega.$$

The above yields

$$(3.19) \quad \begin{bmatrix} c_0(t) \\ c_1(t) \end{bmatrix} = \begin{bmatrix} \cos\left(\frac{\Omega}{2}t\right) & ie^{-i\phi} \sin\left(\frac{\Omega}{2}t\right) \\ ie^{i\phi} \sin\left(\frac{\Omega}{2}t\right) & \cos\left(\frac{\Omega}{2}t\right) \end{bmatrix} \begin{bmatrix} c_0(0) \\ c_1(0) \end{bmatrix}.$$

(Note that if, instead, we relate $C_j(t)$ to $C_j(0)$ for $j = 0, 1$, then because of (3.13), unlike the (special) unitary matrix in (3.19) whose determinant is 1, the corresponding unitary matrix will contain some additional phase factor(s).) Write

$$(3.20) \quad \begin{aligned} \theta &= \frac{\Omega}{2}t \\ \phi' &= \phi + \pi, \end{aligned}$$

and re-name ϕ' as ϕ . Then the above matrix becomes

$$(3.21) \quad U_{\theta, \phi} \equiv \begin{bmatrix} \cos \theta & -ie^{i\phi} \sin \theta \\ -ie^{-i\phi} \sin \theta & \cos \theta \end{bmatrix},$$

which is the *1-bit rotation unitary gate*.

Note that θ in (3.21) depends on t .

REMARK 3.2. If we write the Hamiltonian as ([25, (5.2.44), p. 157])

$$(3.22) \quad H = -\frac{\hbar\Omega}{2}[e^{-i\phi}|1\rangle\langle 0| + e^{i\phi}|0\rangle\langle 1|],$$

then we obtain

$$(3.23) \quad e^{-\frac{i}{\hbar}Ht} = \begin{bmatrix} \cos\left(\frac{\Omega}{2}t\right) & ie^{-i\phi} \sin\left(\frac{\Omega}{2}t\right) \\ ie^{i\phi} \sin\left(\frac{\Omega}{2}t\right) & \cos\left(\frac{\Omega}{2}t\right) \end{bmatrix},$$

which is the same as the matrix in (3.19). This Hamiltonian in (3.22) is thus called the *effective (interaction) Hamiltonian* for the 2-level atom. It represents the essence of the original Hamiltonian in (3.1) after simplifying assumptions. From now on for the many physical systems under discussion, we will simply use the effective Hamiltonians for such systems as supported by theory and/or experiments, rather than to derive the Hamiltonians from scratch based on the Schrödinger's equations coupled with the electromagnetic field. \square

3.2. Quantization of the Electromagnetic Field. The quantization of the electromagnetic radiation field as simple harmonic oscillators is important in quantum optics. This fundamental contribution is due to Dirac. Here we provide a motivation by following the approach of [25, Chap. 1, pp. 3–4]. We begin with the classical description of the field based on Maxwell's equations. These equations relate the electric and magnetic field vectors \mathbf{E} and \mathbf{B} , respectively. Maxwell's equations lead to the following wave equation for the electric field:

$$(3.24) \quad \nabla^2 \mathbf{E} - \frac{1}{c^2} \frac{\partial^2 \mathbf{E}}{\partial t^2} = 0,$$

along with a corresponding wave equation for the magnetic field. The electric field has the spatial dependence appropriate for a cavity resonator of length L . We take the electric field to be linearly polarized in the x -direction and expand in the normal modes (so-called in the sense that they constitute orthogonal coordinates for oscillations) of the cavity

$$(3.25) \quad E_x(z, t) = \sum_j A_j q_j(t) \sin(k_j z),$$

where q_j is the normal mode amplitude with the dimension of a length, $k_j = j\pi/L$, with $j = 1, 2, 3, \dots$, and

$$(3.26) \quad A_j = \left(\frac{2\nu_j^2 m_j}{V\epsilon_0} \right)^{1/2},$$

with $\nu_j = j\pi c/L$ being the cavity eigenfrequency, $V = LA$ (A is the transverse area of the optical resonator) is the volume of the resonator and m_j is a constant with the dimension of mass. The constant m_j has been included only to establish the analogy between the dynamical problem of a single mode of the electromagnetic field and that of the simple harmonic oscillator. The equivalent mechanical oscillator will have a mass m_j , and a Cartesian coordinate q_j . The nonvanishing component of the magnetic field B_y in the cavity is obtained from Eq. (3.25):

$$(3.27) \quad B_y = \sum_j A_j \left(\frac{\dot{q}_j \epsilon_0}{k_j} \right) \cos(k_j z).$$

The classical Hamiltonian for the field is

$$(3.28) \quad H_{cl} = \frac{1}{2} \int_V d\tau (\epsilon_0 E_x^2 + \frac{1}{\mu_0} B_y^2),$$

where the integration is over the volume of the cavity. It follows, on substituting from (3.25) and (3.27) for E_x and B_y , respectively, in (3.28), that

$$(3.29) \quad \begin{aligned} H_{cl} &= \frac{1}{2} \sum_j (m_j \nu_j^2 q_j^2 + m_j \dot{q}_j^2) \\ &= \frac{1}{2} \sum_j \left(m_j \nu_j^2 q_j^2 + \frac{p_j^2}{m_j} \right), \end{aligned}$$

where $p_j = m_j \dot{q}_j$ is the canonical momentum of the j th mode. Equation (3.29) expresses the Hamiltonian of the radiation field as a sum of independent oscillator energies. This suggests correctly that each mode of the field is dynamically equivalent to a mechanical harmonic oscillator.

The present dynamical problem can be quantized by identifying q_j and p_j as operators which obey the commutation relations

$$(3.30) \quad \begin{aligned} [q_j, p_{j'}] &= i\hbar \delta_{jj'}, \\ [q_j, q_{j'}] &= [p_j, p_{j'}] = 0. \end{aligned}$$

In the following we shall restrict ourselves to a single mode of the radiation field modeled by a simple harmonic oscillator. The corresponding Hamiltonian is therefore given by

$$(3.31) \quad H = \frac{1}{2m} p^2 + \frac{1}{2} m \nu^2 x^2,$$

where

$$\begin{aligned}
 p &= \text{the particle momentum operator} = \frac{\hbar}{i} \frac{d}{dx}, \\
 m &= \text{a constant with the dimensions of mass,} \\
 x &= \text{the position operator (corresponding to the } q \text{ variable above),} \\
 \nu &= \text{the natural (circular) frequency of the oscillator} \\
 (3.32) \quad & \text{(a parameter related to the potential depth).}
 \end{aligned}$$

So the eigenstates ψ of the Schrödinger equation satisfy

$$(3.33) \quad H\psi = -\frac{\hbar^2}{2m} \frac{d^2\psi}{dx^2} + \frac{1}{2}m\nu^2 x^2\psi = E\psi.$$

Let us make a change of variables

$$(3.34) \quad y = \sqrt{\frac{m\nu}{\hbar}} x, \quad \lambda = \frac{E}{\hbar\nu},$$

then (3.33) becomes

$$(3.35) \quad \frac{1}{2} \left[\frac{d^2\psi}{dy^2} - y^2\psi \right] = -\lambda\psi.$$

We now define two operators

$$(3.36) \quad a = \frac{1}{\sqrt{2}}(d/dy + y), \quad a^\dagger = -\frac{1}{\sqrt{2}}(d/dy - y).$$

Note that a^\dagger is the Hermitian adjoint operator of a with respect to the $L^2(\mathbb{R})$ inner product. Then it is easy to check that for any sufficiently smooth function ϕ on \mathbb{R} ,

$$(3.37) \quad (aa^\dagger - a^\dagger a)\phi = \phi,$$

i.e.,

$$(3.38) \quad \text{the commutator of } a \text{ with } a^\dagger = [a, a^\dagger] = \mathbf{1},$$

where $\mathbf{1}$ denotes the identity operator but is often simply written as (the scalar) 1 in the physics literature. It is now possible to verify the following:

(i) Let $\tilde{H} \equiv -\frac{1}{2} \left(\frac{d^2}{dy^2} - y^2 \right)$. Then

$$(3.39) \quad \tilde{H} = a^\dagger a + \frac{1}{2}\mathbf{1} = aa^\dagger - \frac{1}{2}\mathbf{1}.$$

(ii) If ψ_λ is an eigenstate of \tilde{H} satisfying

$$(3.40) \quad \tilde{H}\psi_\lambda = \lambda\psi_\lambda \quad (\text{i.e., (3.35)}),$$

then so are $a\psi_\lambda$ and $a^\dagger\psi_\lambda$:

$$\begin{aligned}
 \tilde{H}(a\psi_\lambda) &= (\lambda - 1)a\psi_\lambda, \\
 \tilde{H}(a^\dagger\psi_\lambda) &= (\lambda + 1)a^\dagger\psi_\lambda.
 \end{aligned}$$

(iii) If λ_0 is the lowest eigenvalue (or energy level) of \tilde{H} , then

$$(3.41) \quad \lambda_0 = \frac{1}{2}.$$

(iv) All of the eigenvalues of \tilde{H} are given by

$$(3.42) \quad \lambda_n = \left(n + \frac{1}{2}\right), \quad n = 0, 1, 2, \dots$$

(v) Denote the n -th eigenstate ψ_n by $|n\rangle$, for $n = 0, 1, 2, \dots$. Then

$$(3.43) \quad |n\rangle = \frac{(a^\dagger)^n}{(n!)^{1/2}} |0\rangle.$$

Furthermore,

$$(3.44) \quad \begin{aligned} a^\dagger a |n\rangle &= n |n\rangle, & n &= 0, 1, 2, \dots; \\ a^\dagger |n\rangle &= \sqrt{n+1} |n+1\rangle, & n &= 0, 1, 2, \dots; \\ a |n\rangle &= \sqrt{n} |n-1\rangle, & n &= 1, 2, \dots; \quad a |0\rangle = 0. \end{aligned}$$

(vi) The completeness relation is

$$(3.45) \quad \mathbf{1} = \sum_{n=0}^{\infty} |n\rangle \langle n|.$$

(vii) The wave functions are

$$(3.46) \quad \psi_j(y) = N_j H_j(y) e^{-y^2/2}, \quad y = \left(\frac{m\nu}{\hbar}\right)^{1/2} x,$$

$j = 0, 1, 2, \dots$, where $H_j(y)$ are the Hermite polynomials of degree j , and N_j is a normalization factor,

- REMARK 3.3. (i) The energy levels $(n + \frac{1}{2}) \hbar\nu$ of H (after converting back to the x -coordinate from the y -coordinate in (3.42)) may be interpreted as the presence of n quanta or photons of energy $\hbar\nu$. The eigenstates $|n\rangle$ are called the Fock states or the photon number states.
- (ii) The energy level $E = \frac{1}{2} \hbar\nu$ (from (3.34) and (3.41)) is called the ground state energy.
- (iii) Because of (3.44), we call a and a^\dagger , respectively, the annihilation and creation operators. \square

3.3. Cavity QED for the Quantum Phase Gate. Cavity QED (quantum electrodynamics) is a system that enables the coupling of single atoms to only a few photons in a resonant cavity. It is realized by applying a large laser electric field in a narrow band of frequencies within a small Fabry–Perot cavity consisting of highly reflective mirrors. See a primitive drawing in Fig. 3.2.

A 3-level atom is injected into the cavity. An electron in the atom has three levels, $|\alpha\rangle$, $|\beta\rangle$ and $|\gamma\rangle$, as shown in Fig. 3.3. Actually, the state $|\alpha\rangle$ will be used only as an *auxiliary* level because later we will define the states $|\beta\rangle$ and $|\gamma\rangle$ as the first qubit, $|1\rangle$ and $|0\rangle$, respectively. Once the atom enters the cavity, the strong electromagnetic field of the privileged cavity mode causes transitions of the electron between $|\alpha\rangle$ and $|\beta\rangle$, and a photon or photons are released or absorbed in this process. Of the photon states $|0\rangle$, $|1\rangle$, $|2\rangle$, \dots inside the cavity only $|0\rangle$ and $|1\rangle$ will be important (which physically mean 0 or 1 photo inside the cavity), and they define the second qubit.

The creation and annihilation operators a^\dagger and a act on the photon states $|n\rangle$ for $n = 0, 1, 2, \dots, \infty$, according to (3.44).

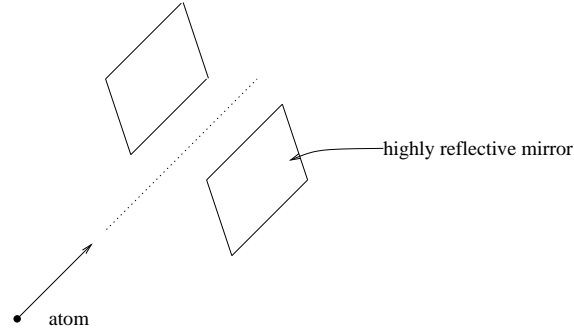


FIGURE 3.2. A Fabry-Perot cavity for electromagnetic radiation. Inside the cavity, the mode structure of the radiation field is drastically changed. In particular, there is a single privileged cavity mode that is resonant with the atomic transition and dominates the atom-field dynamics so completely that the influence of all other modes is negligible.

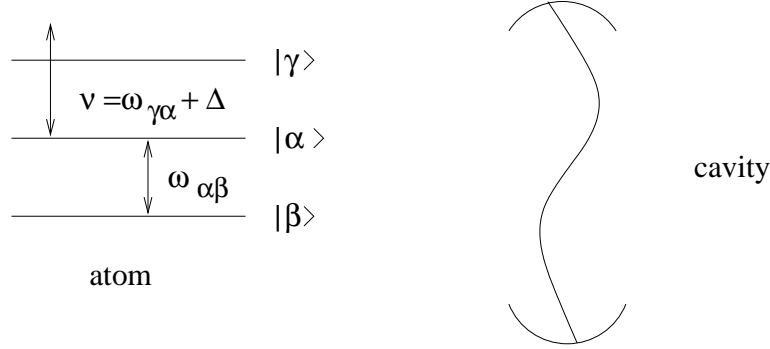


FIGURE 3.3. Diagram for cavity QED.

The Hamiltonian for the atom-cavity field interaction is given by

$$(3.47) \quad H = H_0 + H_1 + H_2,$$

where

$$H_0 = \frac{\hbar\omega_{\alpha\beta}}{2}(|\alpha\rangle\langle\alpha| - |\beta\rangle\langle\beta|) = \text{the atom's Hamiltonian},$$

$$(3.48) \quad H_1 = \hbar\nu a^\dagger a = \text{the Hamiltonian of the laser electric field of the cavity},$$

and

$$(3.49) \quad H_2 = \hbar g(|\alpha\rangle\langle\beta|a + |\beta\rangle\langle\alpha|a^\dagger) = \text{the interaction Hamiltonian of the laser field with the atom; with } g > 0.$$

See the derivation of (3.47) in [21]. Note that the operators a and a^\dagger appearing in (3.47) operate only on the second bit, while the rest of the operators operate only on the first bit. Also, operator $|\alpha\rangle\langle\alpha| - |\beta\rangle\langle\beta|$ can be written as σ_z ; see equation (5.2) later, because its matrix representation with respect to the ordered basis $\{|\alpha\rangle, |\beta\rangle\}$ is exactly σ_z .

LEMMA 3.1. *Let the underlying Hilbert space be*

$$(3.50) \quad \mathcal{H} = \text{span}\{|\alpha, n\rangle, |\beta, n\rangle, |\gamma, n\rangle | n = 0, 1, 2, \dots\}$$

Then the Hamiltonian operator (3.47) has a family of 2-dimensional invariant subspaces

$$(3.51) \quad V_n = \text{span}\{|\alpha, n-1\rangle, |\beta, n\rangle\}, \quad n = 1, 2, \dots$$

Indeed, with respect to the ordered basis in (3.51), the matrix representation of H on V_n is given by

$$(3.52) \quad H|_{V_n} = \hbar \begin{bmatrix} \frac{1}{2}\omega_{\alpha\beta} + \nu(n-1) & g\sqrt{n} \\ g\sqrt{n} & -\frac{1}{2}\omega_{\alpha\beta} + \nu n \end{bmatrix}, \quad n = 1, 2, 3, \dots$$

PROOF. Even though the verification is straightforward, let us provide some details for the ease of future reference. We have, from (3.44), and (3.47)–(3.49),

$$(3.53) \quad \begin{aligned} H|\alpha, n-1\rangle &= H_0|\alpha, n-1\rangle + H_1|\alpha, n-1\rangle + H_2|\alpha, n-1\rangle \\ &= \left[\frac{\hbar\omega_{\alpha\beta}}{2} |\alpha, n-1\rangle \right] + [\hbar\nu(n-1)|\alpha, n-1\rangle] + [\hbar g\sqrt{n}|\beta, n\rangle] \\ &= \hbar \left[\frac{\omega_{\alpha\beta}}{2} + \nu(n-1) \right] |\alpha, n-1\rangle + \hbar[g\sqrt{n}]|\beta, n\rangle. \end{aligned}$$

Similarly,

$$(3.54) \quad H|\beta, n\rangle = \hbar \left[-\frac{\omega_{\alpha\beta}}{2} + \nu n \right] |\beta, n\rangle + \hbar[g\sqrt{n}]|\alpha, n-1\rangle.$$

Therefore, we obtain (3.52). \square

LEMMA 3.2. *On the invariant subspace V_n in (3.51), the Hamiltonian operator H has two eigenstates*

$$(3.55) \quad \begin{cases} |+\rangle_n \equiv \cos\theta_n |\alpha, n-1\rangle - \sin\theta_n |\beta, n\rangle, \\ |-\rangle_n \equiv \sin\theta_n |\alpha, n-1\rangle + \cos\theta_n |\beta, n\rangle, \end{cases}$$

where

$$(3.56) \quad \begin{aligned} \sin\theta_n &\equiv \frac{\Omega_n - \Delta}{D}, \quad \cos\theta_n \equiv \frac{2g\sqrt{n}}{D}, \\ D &\equiv [(\Omega_n - \Delta)^2 + 4g^2n]^{1/2}, \\ \Omega_n &\equiv (\Delta^2 + 4g^2n)^{1/2}, \\ \Delta &\equiv \nu - \omega_{\alpha\beta} = \text{the detuning frequency}, \end{aligned}$$

with eigenvalues (i.e., energy levels)

$$(3.57) \quad E_{\pm(n)} = \hbar \left[n\nu + \frac{1}{2}(-\nu \mp \Omega_n) \right],$$

such that

$$(3.58) \quad H|+\rangle_n = E_{+(n)}|+\rangle_n, \quad H|-\rangle_n = E_{-(n)}|-\rangle_n.$$

PROOF. These eigenvalues and eigenvectors can be computed in a straightforward way, using the 2×2 matrix representation of H on V_n , (3.52), with respect to the ordered basis of V_n chosen as in (3.51). \square

REMARK 3.4. The states $|+\rangle_n$ and $|-\rangle_n$ in (3.55) are called the *dressed states* in the sense that atoms are dressed by electromagnetic fields. These two states are related to the splitting of the spectral lines due to the electric field. \square

Now, let us assume *large detuning*:

$$(3.59) \quad |\Delta| \gg 2g\sqrt{n}.$$

Also, $|\Delta|$ remains small in comparison to the transition frequency so that approximate resonance is maintained. Accordingly, this is satisfied only for small values of n . Then

$$(3.60) \quad \begin{aligned} \Omega_n &= (\Delta^2 + 4g^2n)^{1/2} = \Delta \left(1 + \frac{2g^2n}{\Delta^2}\right)^{1/2} \approx \Delta + \frac{2g^2n}{\Delta}; \\ \sin \theta_n &= (\Omega_n - \Delta)/D \approx 0; \quad \cos \theta_n = 2g\sqrt{n}/D \approx 1. \end{aligned}$$

Thus, from (3.55),

$$(3.61) \quad |+\rangle_n \approx |\alpha, n-1\rangle, \quad |-\rangle_n \approx |\beta, n\rangle.$$

REMARK 3.5. By the assumption (3.58) of large detuning, from (3.57) using (3.56) and (3.59), we now have

$$(3.62) \quad \begin{aligned} E_{+(n)} &= \hbar \left[n\nu + \frac{1}{2}(-\nu - \Omega_n) \right] \\ &\approx \hbar \left[\left(n - \frac{1}{2}\right) \nu - \frac{1}{2} \left(\Delta + \frac{2g^2n}{\Delta} \right) \right] \\ &= \hbar \left[\left(n - \frac{1}{2}\right) \nu - \frac{1}{2}(\nu - \omega_{\alpha\beta}) - \frac{g^2n}{\Delta} \right] \\ &= \hbar \left[\frac{\omega_{\alpha\beta}}{2} + \nu(n-1) \right] - \frac{\hbar g^2n}{\Delta}. \end{aligned}$$

Similarly, we have

$$(3.63) \quad E_{-(n)} \approx \hbar \left[-\frac{\omega_{\alpha\beta}}{2} + \nu n \right] + \frac{\hbar g^2n}{\Delta},$$

such that

$$(3.64) \quad \begin{aligned} H|+\rangle_n &\approx H|\alpha, n-1\rangle = E_{+(n)}|\alpha, n-1\rangle, \\ H|-\rangle_n &\approx H|\beta, n\rangle = E_{-(n)}|\beta, n\rangle, \end{aligned}$$

where $E_{\pm(n)}$ are now given by (3.62) and (3.63).

Thus, we see that the assumption (3.58) of large detuning causes the off-diagonal terms in the matrix (3.52) (which are contributed by the *interaction Hamiltonian* H_2 in (3.48)) to disappear. The de facto or, *effective interaction Hamiltonian*, has now become

$$(3.65) \quad \tilde{H}_2 = -\frac{\hbar g^2}{\Delta} (aa^\dagger|\alpha\rangle\langle\alpha| - a^\dagger a|\beta\rangle\langle\beta|),$$

such that $\tilde{H} \equiv H_0 + H_1 + \tilde{H}_2$ now admits a diagonal matrix representation

$$(3.66) \quad \tilde{H}|_{V_n} = \begin{bmatrix} E_{+(n)} & 0 \\ 0 & E_{-(n)} \end{bmatrix}$$

with respect to the ordered basis $\{|\alpha, n-1\rangle, |\beta, n\rangle\}$ of V_n , with $E_{\pm(n)}$ here given by (3.62) and (3.63). \square

We now define the first qubit by

$$(3.67) \quad |\beta\rangle = |1\rangle, \quad |\gamma\rangle = |0\rangle,$$

where $|\gamma\rangle$ is the state in Fig. 3.3 that is *detached* (or *off-resonance*) from the Hamiltonian H , i.e.,

$$(3.68) \quad H|\gamma\rangle = 0.$$

For the second qubit, we choose $n = 1$ for V_n in (3.51) and then see that the second bit is only 0 or 1, i.e., the cavity can have 0 or 1 photon. The cavity field is nearly resonant with the $|\alpha\rangle \leftrightarrow |\beta\rangle$ transition: $\nu = \omega_{\alpha\beta} + \Delta$.

THEOREM 3.3. *Let the effective total Hamiltonian be*

$$(3.69) \quad \begin{aligned} \tilde{H} = H_0 + H_1 + \tilde{H}_2 = \hbar \left[\frac{\omega_{\alpha\beta}}{2} (|\alpha\rangle\langle\alpha| - |\beta\rangle\langle\beta|) + \nu a^\dagger a \right. \\ \left. - \frac{\hbar g^2}{\Delta} (a a^\dagger |\alpha\rangle\langle\alpha| - a^\dagger a |\beta\rangle\langle\beta|) \right]. \end{aligned}$$

Then

$$(3.70) \quad \tilde{V} \equiv \text{span}\{|0, 0\rangle, |0, 1\rangle, |1, 0\rangle, |1, 1\rangle\}$$

is an invariant subspace of \tilde{H} in the underlying Hilbert space (3.50), such that

$$(3.71) \quad \begin{cases} \tilde{H}|0, 0\rangle = 0, & \tilde{H}|0, 1\rangle = 0, & \tilde{H}|1, 0\rangle = 0 \\ \tilde{H}|1, 1\rangle = E_{-(1)}|1, 1\rangle, & \text{where } E_{-(1)} = \hbar \left(-\frac{\omega_{\alpha\beta}}{2} + \nu + \frac{\hbar g^2}{\Delta} \right). \end{cases}$$

Consequently, with respect to the ordered basis of \tilde{V} in (3.70), \tilde{H} admits a diagonal matrix representation

$$(3.72) \quad \tilde{H}|_{\tilde{V}} = \begin{bmatrix} 0 & & & \circ \\ & 0 & & \\ & & 0 & \\ \circ & & & E_{-(1)} \end{bmatrix},$$

with the evolution operator

$$(3.73) \quad e^{-i\tilde{H}t/\hbar}|_{\tilde{V}} = \begin{bmatrix} 1 & & & \\ & 1 & & \circ \\ & & 1 & \\ \circ & & & \exp\left(-i\frac{E_{-(1)}t}{\hbar}\right) \end{bmatrix}.$$

PROOF. We have

$$(3.74) \quad \tilde{H}|0, 0\rangle = \tilde{H}|\gamma, 0\rangle = 0 \quad \text{and} \quad \tilde{H}|0, 1\rangle = \tilde{H}|\gamma, 1\rangle = 0, \quad \text{by (3.68).}$$

Also,

$$(3.75) \quad \tilde{H}|1, 0\rangle = \tilde{H}|\beta, 0\rangle = 0, \quad \text{by (3.66),}$$

where V_n is chosen to be V_0 by setting $n = 0$ therein. But

$$(3.76) \quad \tilde{H}|1, 1\rangle = \tilde{H}|\beta, 1\rangle = E_{-(1)}|1, 1\rangle$$

by (3.66) where V_n is chosen to be V_1 by setting $n = 1$ therein. So both (3.72) and (3.73) follow. \square

The unitary operator in (3.73) gives us the quantum phase gate

$$(3.77) \quad Q_\eta = \begin{bmatrix} 1 & & & \\ & 1 & & \bigcirc \\ & & 1 & \\ & \bigcirc & & e^{i\phi} \end{bmatrix}$$

with

$$(3.78) \quad \phi \equiv -\frac{E_{-(1)}}{\hbar}t.$$

We can now invoke Theorem 2.2 in Section 2 to conclude the following.

THEOREM 3.4. *The collection of 1-bit gates $U_{\theta,\phi}$ in (3.21) from the 2-level atoms and the 2-bit gates Q_η in (3.77) from cavity QED is universal for quantum computation.* \square

4. Ion Traps

Ion traps utilize charged atoms with internal electronic states to represent qubits. Ion traps isolate and confine small numbers of charged atoms by means of electromagnetic fields. The ions are then cooled using laser beams until their kinetic energy is much smaller than the inter-ionic potential energy. Under these conditions, the ions form a regular array in the trap. Laser beams can be tuned to excite the electronic states of particular ions and to couple these internal states to the center-of-mass (CM) vibrational motion of the ion array. This coupling provides entanglement for quantum computation.

A Paul, or radio-frequency, ion trap confines ions by the time average of an oscillating force $F(\mathbf{r}, t)$, where $\mathbf{r} = (x, y, z)$, arising from a non-uniform electric field $E(\mathbf{r}) \cos(\mu t)$ acting on the ion charge e with mass m . In one dimension, $\langle F(X, t) \rangle = -\partial \langle U(X, t) \rangle / \partial X$, where $\langle U(X, t) \rangle$ is an effective time-averaged potential energy, and $U(X, t) = e^2 E^2(X) \cos^2(\Omega t) / (m \Omega^2)$. The time average is denoted by $\langle \rangle$ and here, it is defined by $\langle y(t) \rangle = \frac{\Omega}{2\pi} \int_0^{2\pi/\Omega} y(t) dt$, where $y(t)$ is periodic with period $2\pi/\Omega$. X describes the (relatively slow) motion of a guiding center, about which the ions execute small oscillations at frequency Ω . The trap is constructed so that the guiding center motion in two dimensions (say x and y) is harmonic, with frequencies ν_x and ν_y which are much smaller than the frequency Ω . The trap electrodes may confine the ions in a circle or other closed 2-dimensional geometry, or a linear trap may be produced by using a dc potential to confine the ions in the third spatial dimension z ; see Fig. 4.1.

Once confined in the trap, the ions may be cooled using laser light, so that they condense into a linear array along the trap axis. Each ion oscillates with small amplitude about the zero of the time-averaged radial potential. The electrostatic repulsion of the ions along the linear axis of the trap combats a spatially varying dc potential applied for axial confinement, so that below milliKelvin ($1 \times 10^{-3} K$) temperatures, the ions in the array are separated by several micrometers ($10^{-6} m$). Under these conditions, the ion confinement time is very long, many hours or days, and each ion can be separately excited by a focused laser beam, so that long-lived

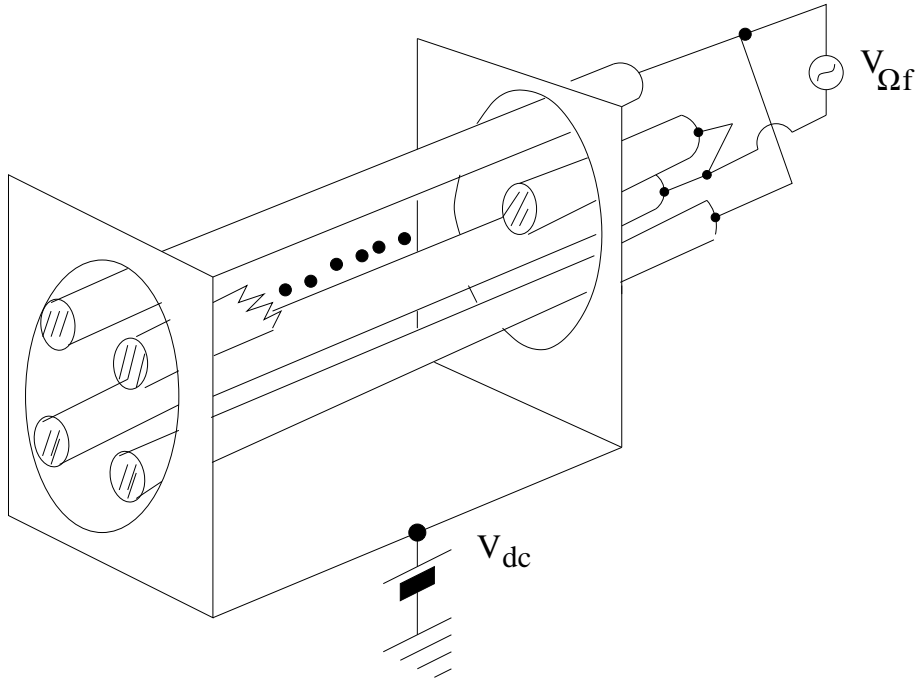


FIGURE 4.1. Diagram of a linear ion trap, showing the radio-frequency voltage connections on the four rods of the trap, and the dc voltage connection for an axial dc potential well. One rod is partially cut back to reveal 6 cold ions (hiding behind, not inside, the rod) confined in a linear array within the trap. The ions would be visible due to scattered light, if they were all simultaneously excited by a laser beam tuned to an internal resonance transition, at a wavelength in the visible region of the spectrum. The separation of the trap rods is on the order of a millimeter.

internal levels of each ion can serve as the two states of a qubit (Fig. 4.2). Regarding the axial kinetic motion, the ions oscillate axially as a group, so collective oscillations such as the CM oscillations couple the individual ions, or qubits, permitting the implementation of multi-qubit gates based on quantum entanglement of the CM motion with each laser-excited qubit state. There are many CM modes of oscillation, depending on the oscillations of individual ions or groups of ions, each with a characteristic frequency ω_{CM} .

A prototype scheme was proposed by Cirac and Zoller [7], which is based on a confined ion system as outlined above. Assume the quantized axial CM normal mode oscillation has frequency ω_{CM} and discrete levels $n\hbar\omega_{\text{CM}}$ with quantum number $n = 0, 1, 2, \dots$ (the ground state zero-point energy $\hbar\omega_{\text{CM}}/2$ in Remark 3.3(ii) is disregarded); see Fig. 4.3(b). A quantum of oscillation $\hbar\omega_{\text{CM}}$ is called a *phonon*. Each ion is individually excited by focused standing wave laser beams. Two internal hyperfine structure states of the ion (i.e., states coupling the electrons and the nucleus of the ion) in the ground term (or lowest electronic set of states), separated by the frequency ω_0 , can be identified as the qubit states $|0\rangle$ and $|1\rangle$. Alternatively,

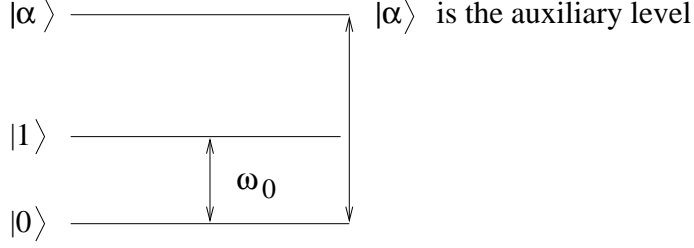


FIGURE 4.2. Diagram of the energy levels of an idealized ion, which might serve as the two qubit levels, plus an auxiliary level used in a particular implementation of a quantum circuit. The actual levels of a real ion are much more complex, but approximate the ideal case when the exciting lasers are properly tuned.

a ground level and a metastable excited level might be used. By thus coupling only these selected states of the ion by electromagnetic fields we are led to a *2-level atom* analogously as in Section 3. These states can be coupled using electric dipole transitions to higher-lying states, and there is also an internal auxiliary level, denoted $|\alpha\rangle$, which can be coupled to the qubit states; see Fig. 4.2. Consequently a linear N -ion system can be specified in terms of quantum numbers by the wavefunction $|\psi\rangle_N = |j_1\rangle|j_2\rangle \cdots |j_N\rangle|k\rangle_{\text{CM}}$, where states (of each ion) $j_1, j_2, \dots, j_N \in \{0, 1\}$ and $k = 0, 1, 2, \dots, N - 1$ describes the populated quantum state of the CM motion. The system is initialized with $k = 0$ when the ions are very cold, and with all qubit states j_1, j_2, \dots, j_N set to 0 by inducing appropriate laser transitions in the individual ions.

Fig. 4.3(b) gives a diagram of the harmonic potential well of the axial ion center-of-mass vibration, showing the lowest energy levels. The six ions in Fig. 4.3(a) would populate one of these energy levels, acting as a single entity with the CM coordinates.

The acting laser beam tuned to frequency ω_0 causes a dipole transition coupling the two qubit levels $|0\rangle$ and $|1\rangle$ in Fig. 4.2. Using the same rotating wave approximation as in Section 3, we obtain the 1-bit rotation matrix $U_{\theta, \phi}$ as in (3.21).

Therefore, according to the theory of universal quantum computing (Theorem 2.1) in Section 2, now all we need to show is an entanglement operation between two qubits.

We assume that two ions corresponding to the two qubits are coupled in the *Lamb-Dicke regime*, i.e., the amplitude of the ion oscillation in the ion trap potential is small compared to the wavelength of the incident laser beam. This is expressed in terms of the Lamb-Dicke criterion:

$$(4.1) \quad \eta(\Omega/2\omega_{\text{CM}}) \ll 1$$

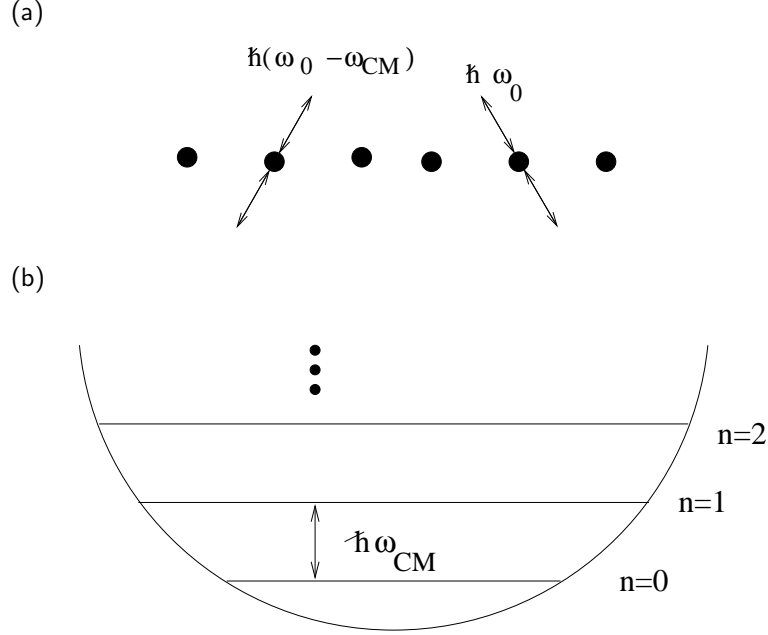


FIGURE 4.3. (a) A diagram showing 6 cold ions in a linear array. the arrows show two of the ions individually excited by focused laser beam standing waves. One laser is tuned to the internal qubit transition frequency ω_0 , while the other laser is tuned to the first red sideband frequency $\omega_0 - \omega_{CM}$, which couples the internal transition to the center-of-mass vibration of the ion array at ω_{CM} in the ion trap.

(b) A diagram of the harmonic potential well of the axial ion center-of-mass vibration, showing the lowest energy levels. The six ions in (a) would populate one of these energy levels, acting as a single entity with the CM coordinates.

where

$$\begin{aligned}
 (4.2) \quad & \eta \equiv kz_0 : \text{ the Lamb-Dicke parameter,} \\
 & \quad z_0 : \text{ a "zero-point" oscillation amplitude,} \\
 & \quad \quad \text{at the lowest energy of CM vibration,} \\
 & k = 2\pi/\lambda : \text{ the wave number of the laser radiation,} \\
 & \omega_{CM} : \text{ the frequency of the CM motion referred to earlier,} \\
 & \Omega : \text{ the Rabi frequency (cf. (3.11)).}
 \end{aligned}$$

When (4.1) is satisfied, the "sideband" frequencies $\omega_0 \pm \omega_{CM}$ arising from the CM oscillation in the laser standing wave are *resolved* (see Fig. 4.4 and the captions therein), and can be separately excited by the laser beam; see Fig. 4.3(a). Then the interaction Hamiltonian coupling the internal qubit states of each ion j , $j =$

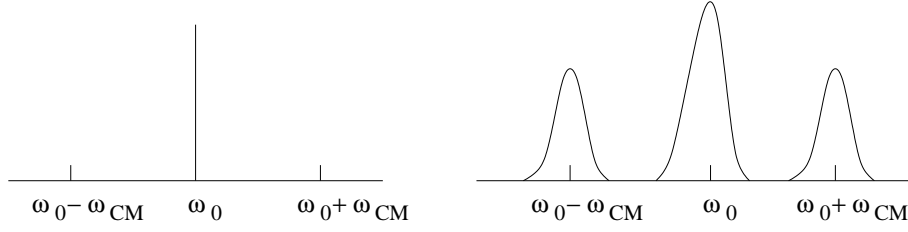


FIGURE 4.4. $\omega_0 - \omega_{\text{CM}}$ is the red sideband frequency which may be excited to entangle the qubit with the CM motion. The right figure indicates that when the Lamb–Dicke criterion is satisfied the sideband frequencies $\omega_0 \pm \omega_{\text{CM}}$ and ω_0 , which have finite widths due to the Heisenberg uncertainty principle, are resolved, enabling separate excitations by the laser beam. (The frequency $\omega_0 + \omega_{\text{CM}}$ is called the blue sideband frequency; see [28].)

$1, \dots, N$, to the CM motion is similar to (3.49), with coupling constant $g = \frac{\eta\Omega}{2\sqrt{N}}$:

$$(4.3) \quad H_j = \frac{\hbar\eta\Omega}{2\sqrt{N}} [|1\rangle_j \langle 0|_j e^{-i\phi} a + |0\rangle_j \langle 1|_j e^{i\phi} a^\dagger], \quad j = 1, \dots, N,$$

where a and a^\dagger are, respectively, the annihilation and creation operators (see Subsection 3.2) for the phonons defined by

$$(4.4) \quad \begin{aligned} a|n\rangle_{\text{CM}} &= \sqrt{n} |n-1\rangle_{\text{CM}}, \text{ for } n = 1, 2, \dots; \quad a|0\rangle_{\text{CM}} = 0|0\rangle_{\text{CM}} = 0, \\ a^\dagger|n\rangle_{\text{CM}} &= \sqrt{n+1} |n+1\rangle_{\text{CM}}, \text{ for } n = 0, 1, 2, \dots; \text{ cf. (3.44),} \end{aligned}$$

and

$$(4.5) \quad \begin{aligned} \phi &= \text{the angle in the spherical coordinate system } (r, \theta, \phi) \text{ with respect} \\ &\text{to the } x\text{-axis of the laboratory coordinate frame.} \end{aligned}$$

The derivations of (4.3) may be found in [14, Section 5.1] where the authors give an argument based on normal modes of phonons. At low enough temperature (i.e., the Lamb–Dicke regime), only the lowest order or the CM mode plays a role, and this leads to the Hamiltonian (4.3) used by Cirac and Zoller in [7].

REMARK 4.1. It can be shown that the Rabi frequency Ω_R for the internal qubit transition coupled by a and a^\dagger to the vibration is $\eta\Omega/(2\sqrt{N})$, much smaller than that, Ω , in (3.11) for a single qubit (rotation) operation. \square

LEMMA 4.1. *Let H_j be given by (4.3) for $j = 1, 2, \dots, N$. Then H_j has a family of invariant two-dimensional subspaces*

$$(4.6) \quad V_{j,k} \equiv \text{span}\{|0\rangle_j |k+1\rangle_{\text{CM}}, |1\rangle_j |k\rangle_{\text{CM}}\}, \quad k = 0, 1, 2, \dots,$$

in the Hilbert space

$$(4.7) \quad V_j \equiv \text{span}\{|0\rangle_j |k\rangle_{\text{CM}}, |1\rangle_j |k\rangle_{\text{CM}} \mid k = 0, 1, 2, \dots\}.$$

On the orthogonal complement of all the $V_{j,k}$'s, i.e., $\tilde{V}_j = \left(\text{span} \bigcup_{k=0}^{\infty} V_{j,k} \right)^\perp \subset V_j$, the action of H_j is 0: $H_j|\psi\rangle = 0$ for all $\psi \in \tilde{V}_j$.

PROOF. We have

$$\begin{aligned}
 H_j |0\rangle_j |k+1\rangle_{\text{CM}} &= \frac{\hbar\eta\Omega}{2\sqrt{N}} [|1\rangle_j \langle 0|_j e^{-i\phi} (a|k+1\rangle_{\text{CM}}) + |0\rangle_j \langle 1|_j e^{i\phi} (a^\dagger|k+1\rangle_{\text{CM}})] \\
 (4.8) \quad &= \frac{\hbar\eta\Omega}{2\sqrt{N}} e^{-i\phi} \sqrt{k+1} |1\rangle_j |k\rangle_{\text{CM}},
 \end{aligned}$$

and, similarly,

$$(4.9) \quad H_j |1\rangle_j |k\rangle_{\text{CM}} = \frac{\hbar\eta\Omega}{2\sqrt{N}} e^{i\phi} \sqrt{k+1} |0\rangle_j |k+1\rangle_{\text{CM}}.$$

Thus, $V_{j,k}$ is an invariant two-dimensional subspace of H_j in V_j . \square

Let the time-evolution operator of H_j (depending on ϕ) on V_j be $U_j(t, \phi) = e^{-\frac{i}{\hbar} H_j t}$. Then on the subspace $V_{j,k}$, $k = 0, 1, 2, \dots, \infty$, with respect to the ordered basis $\{|0\rangle_j |k+1\rangle_{\text{CM}}, |1\rangle_j |k\rangle_{\text{CM}}\}$, H_j admits the following matrix representation

$$(4.10) \quad H_j = \frac{\hbar\eta\Omega}{2} \sqrt{\frac{k+1}{N}} \begin{bmatrix} 0 & e^{-i\phi} \\ e^{i\phi} & 0 \end{bmatrix}.$$

Thus, with H_j restricted to $V_{j,k}$, its time-evolution operator is given by

$$\begin{aligned}
 (4.11) \quad U_{j,k}(t, \phi) &\equiv U_j(t, \phi)|_{V_{j,k}} = e^{-\frac{i}{\hbar} H_j t} \Big|_{V_{j,k}} \\
 &= \begin{bmatrix} \cos(\mathcal{E}_k t) & -ie^{-i\phi} \sin(\mathcal{E}_k t) \\ -ie^{i\phi} \sin(\mathcal{E}_k t) & \cos(\mathcal{E}_k t) \end{bmatrix}, \quad \mathcal{E}_k \equiv \frac{\hbar\eta\Omega}{2} \sqrt{\frac{k+1}{N}}.
 \end{aligned}$$

Also, note that

$$(4.12) \quad U_j(t, \phi)|\psi\rangle = |\psi\rangle \quad \text{for all } |\psi\rangle \in \tilde{V}_j,$$

because the action of H_j on \tilde{V}_j is annihilation. In physics, these states in \tilde{V}_j are said to be *off-resonance*.

Next, define

$$(4.13) \quad H_j^{\text{aux}} = \frac{\hbar\eta\Omega}{2\sqrt{N}} [|\alpha\rangle_j \langle 0|_j e^{-i\phi} a + |0\rangle_j \langle \alpha|_j e^{i\phi} a^\dagger], \quad j = 1, 2,$$

where $|\alpha\rangle$ is the auxiliary quantum state as indicated in Fig. 4.2. Then, similarly to Lemma 4.1, we have the following.

LEMMA 4.2. *Let H_j^{aux} be given by (4.13) for $j = 1, 2, \dots, N$. Then H_j^{aux} has a family of invariant two-dimensional subspaces*

$$(4.14) \quad V_{j,k}^{\text{aux}} \equiv \text{span}\{|0\rangle_j |k+1\rangle_{\text{CM}}, |\alpha\rangle_j |k\rangle_{\text{CM}}\}, \quad k = 0, 1, 2, \dots,$$

in the Hilbert space

$$(4.15) \quad V_j^{\text{aux}} \equiv \text{span}\{|0\rangle_j |k\rangle_{\text{CM}}, |\alpha\rangle_j |k\rangle_{\text{CM}} \mid k = 0, 1, 2, \dots\}.$$

On the orthogonal complement $\tilde{V}_j^{\text{aux}} \equiv \left(\text{span} \bigcup_{k=0}^{\infty} V_{j,k}^{\text{aux}} \right)^\perp \subset V_j^{\text{aux}}$, the action of H_j^{aux} is 0: $H_j^{\text{aux}}|\psi\rangle = 0$ for all $|\psi\rangle \in \tilde{V}_j^{\text{aux}}$. \square

The time-evolution operator corresponding to H_j^{aux} on V_j^{aux} is denoted as $U_j^{\text{aux}}(t, \phi) = e^{-\frac{i}{\hbar} H_j^{\text{aux}} t}$. Now, restrict H_j^{aux} to the invariant two-dimensional subspace $V_{j,k}^{\text{aux}}$ with ordered basis $\{|0\rangle_j |k+1\rangle_{\text{CM}}, |\alpha\rangle_j |k\rangle_{\text{CM}}\}$; its evolution operator has the matrix representation

$$(4.16) \quad \begin{aligned} U_{j,k}^{\text{aux}}(t, \phi) &\equiv U_j^{\text{aux}}(t, \phi)|_{V_{j,k}^{\text{aux}}} = e^{-\frac{i}{\hbar} H_j^{\text{aux}} t}|_{V_{j,k}^{\text{aux}}} \\ &= \begin{bmatrix} \cos(\mathcal{E}_k t) & -ie^{-i\phi} \sin(\mathcal{E}_k t) \\ -ie^{i\phi} \sin(\mathcal{E}_k t) & \cos(\mathcal{E}_k t) \end{bmatrix}, \quad \mathcal{E}_k \equiv \frac{\hbar\eta\Omega}{2} \sqrt{\frac{k+1}{N}}. \end{aligned}$$

Here, we again also have

$$(4.17) \quad U_j^{\text{aux}}(t, \phi)|\psi\rangle = |\psi\rangle \quad \text{for all } |\psi\rangle \in \tilde{V}_j^{\text{aux}},$$

because H_j^{aux} annihilates the subspace \tilde{V}_j^{aux} . Using the CM mode as the bus, we can now derive the following 2-bit quantum phase gate.

THEOREM 4.3. *Let $U_j(t, \phi), U_{j,k}(t, \phi), U_j^{\text{aux}}(t, \phi)$ and $U_{j,k}^{\text{aux}}(t, \phi)$ be defined as above satisfying (4.11)–(4.17) for $j = 1, 2$ and $k = 0$. Then for*

$$(4.18) \quad U \equiv U_1(T, 0)U_2^{\text{aux}}(2T, 0)U_1(T, 0), \quad T \equiv \frac{\pi}{\eta\Omega} \sqrt{N},$$

we have

$$(4.19) \quad U|0\rangle_1|0\rangle_2|0\rangle_{\text{CM}} = |0\rangle_1|0\rangle_2|0\rangle_{\text{CM}},$$

$$(4.20) \quad U|1\rangle_1|0\rangle_2|0\rangle_{\text{CM}} = |1\rangle_1|0\rangle_2|0\rangle_{\text{CM}},$$

$$(4.21) \quad U|0\rangle_1|1\rangle_2|0\rangle_{\text{CM}} = |0\rangle_1|1\rangle_2|0\rangle_{\text{CM}},$$

$$(4.22) \quad U|1\rangle_1|1\rangle_2|0\rangle_{\text{CM}} = -|1\rangle_1|1\rangle_2|0\rangle_{\text{CM}}.$$

Consequently, by ignoring the last CM-bit $|0\rangle_{\text{CM}}$, we have the phase gate

$$(4.23) \quad U = Q_\pi, \quad \text{cf. (2.18)}.$$

PROOF. We first verify (4.19):

$$(4.24) \quad \begin{aligned} U|0\rangle_1|0\rangle_2|0\rangle_{\text{CM}} &= U_1(T, 0)U_2^{\text{aux}}(2T, 0)[U_1(T, 0)|0\rangle_1|0\rangle_{\text{CM}}]|0\rangle_2 \\ &= U_1(T, 0)U_2^{\text{aux}}(2T, 0)[|0\rangle_1|0\rangle_{\text{CM}}]|0\rangle_2 \\ &\quad (\text{by (4.12) because } |0\rangle_1|0\rangle_{\text{CM}} \in \tilde{V}_j \text{ for } j = 1) \\ &= U_1(T, 0)[U_2^{\text{aux}}(2T, 0)|0\rangle_2|0\rangle_{\text{CM}}]|0\rangle_1 \\ &= U_1(T, 0)[|0\rangle_2|0\rangle_{\text{CM}}]|0\rangle_1 \\ &\quad (\text{by (4.17) because } |0\rangle_2|0\rangle_{\text{CM}} \in \tilde{V}_j^{\text{aux}} \text{ for } j = 2) \\ &= [U_1(T, 0)|0\rangle_1|0\rangle_{\text{CM}}]|0\rangle_2 \\ &= |0\rangle_1|0\rangle_{\text{CM}}|0\rangle_2 \\ &\quad (\text{by (4.12) because } |0\rangle_2|0\rangle_{\text{CM}} \in \tilde{V}_j \text{ for } j = 1) \\ &= |0\rangle_1|0\rangle_2|0\rangle_{\text{CM}}. \end{aligned}$$

Next, we verify (4.20):

$$\begin{aligned}
 U|1\rangle_1|0\rangle_2|0\rangle_{\text{CM}} &= U_1(T, 0)U_2^{\text{aux}}(2T, 0)[U_1(T, 0)|1\rangle_0|0\rangle_{\text{CM}}]|0\rangle_2 \\
 &= U_1(T, 0)U_2^{\text{aux}}(2T, 0)[-i|0\rangle_1|1\rangle_{\text{CM}}]|0\rangle_2 \\
 &\quad (\text{using (4.11) with } k=0, \phi=0 \text{ and } \mathcal{E}_k T = \pi/2) \\
 &= U_1(T, 0)\{(-i)[U_2(2T, 0)|0\rangle_2|1\rangle_{\text{CM}}]|0\rangle_1\} \\
 &= U_1(T, 0)\{[i|0\rangle_2|1\rangle_{\text{CM}}]|0\rangle_1\} \\
 &\quad (\text{using (4.16) and (4.11) with } k=0, \phi=0 \text{ and } 2\mathcal{E}_k T = \pi) \\
 &= i[U_1(T, 0)|0\rangle_1|1\rangle_{\text{CM}}]|0\rangle_2 \\
 &= i[(-i)|1\rangle_1|0\rangle_{\text{CM}}]|0\rangle_2 \\
 &\quad (\text{using (4.11) with } k=0, \phi=0 \text{ and } \mathcal{E}_k T = \pi/2) \\
 (4.25) \quad &= |1\rangle_1|0\rangle_2|0\rangle_{\text{CM}}.
 \end{aligned}$$

The verification of (4.21) can be done in the same way as that for (4.19).

Finally, we verify (4.22):

$$\begin{aligned}
 U|1\rangle_1|1\rangle_2|0\rangle_{\text{CM}} &= U_1(T, 0)U_2^{\text{aux}}(2T, 0)[U_1(T, 0)|1\rangle_1|0\rangle_{\text{CM}}]|1\rangle_2 \\
 &= U_1(T, 0)U_2^{\text{aux}}(2T, 0)[-i|0\rangle_1|1\rangle_{\text{CM}}]|1\rangle_2 \\
 &\quad (\text{using (4.11) with } j=1, k=0, \phi=0 \text{ and } \mathcal{E}_k T = \pi/2) \\
 &= U_1(T, 0)[(-i)U_2^{\text{aux}}(2T, 0)|1\rangle_2|1\rangle_{\text{CM}}]|0\rangle_1 \\
 &= U_1(T, 0)[(-i)|1\rangle_2|1\rangle_{\text{CM}}]|0\rangle_1 \\
 &\quad (\text{by (4.17) because } |1\rangle_2|1\rangle_{\text{CM}} \in \widetilde{V}_j^{\text{aux}} \text{ for } j=2) \\
 &= (-i)[U_1(T, 0)|0\rangle_1|1\rangle_{\text{CM}}]|1\rangle_2 \\
 &= (-i)[(-i)|1\rangle_1|0\rangle_{\text{CM}}]|1\rangle_2 \\
 &\quad (\text{using (4.11) with } j=1, k=0, \phi=0 \text{ and } \mathcal{E}_k T = \pi/2) \\
 (4.26) \quad &= -|1\rangle_1|1\rangle_2|0\rangle_{\text{CM}}.
 \end{aligned}$$

The verifications are complete. \square

The CNOT gate can now be obtained according to Corollary 2.3. As a consequence, we have the following.

THEOREM 4.4. *The quantum computer made of confined ions in a trap is universal.*

PROOF. Use (2.19) and (4.23) to deduce Corollary 2.3. \square

A very similar gate has been implemented experimentally using a cold, confined Be^+ ion [19]. To conclude this section, we mention two more schemes using ion traps.

(a) The Sørensen–Mølmer scheme [26].

Experimental inconveniences in implementation of the Cirac–Zoller scheme on confined ions include the requirement that the ions be initialized in the ground vibrational state $|0\rangle_{\text{CM}}$, which requires sophisticated laser cooling techniques, and the experimental observation that the CM vibration of a linear string of ions in a trap has limited coherence. The Sørensen–Mølmer scheme applies to a string of ions, but the ions can have thermal motion, as long as they remain within the

Lamb–Dicke regime. The ions never populate a vibrational mode, so decoherence effects are reduced. The idea is to simultaneously excite an ion *pair* using two laser beams detuned by frequency δ from the upper and lower vibrational sidebands $\omega_0 + \omega_{\text{CM}} - \delta$ and $\omega_0 - \omega_{\text{CM}} + \delta$, so that the energy (or frequency) sum is $2\omega_0$, corresponding to excitation of both ions by two interfering transition paths from $|0, 0\rangle|n\rangle$ to $|1, 1\rangle|n\rangle$, without changing the vibrational state. The lasers are detuned from the red and blue sideband transitions of *single* ion excitation, so the vibration is only virtually (negligibly) excited, and the vibration levels are never actually populated. One laser beam is applied to each ion. For any two ions, each illuminated by *both* of the laser beams, an additional two interference paths exist, and the effective Rabi frequency for the two-ion transition becomes $\Omega_{\text{SM}} = -(\eta\Omega)^2/(\omega_{\text{CM}} - \delta)$, where Ω represents the single ion Rabi frequency at the same laser power. The two-ion interaction Hamiltonian can be written $(\hbar\Omega_{\text{SM}}/2)(|0, 0\rangle\langle 1, 1| + |1, 1\rangle\langle 0, 0| + |1, 0\rangle\langle 0, 1| + |0, 1\rangle\langle 1, 0|)$. The Rabi frequency can be approximated as $\Omega_{\text{SM}} = \eta^2\Omega^2/\delta$, since $\omega_{\text{CM}} - \delta \approx \delta$. Full entanglement is achieved at a particular interaction time $T = \pi/2\Omega_{\text{SM}}$, when the wavefunction becomes a coherent superposition of maximally entangled $|0, 0\rangle$ and $|1, 1\rangle$ states $|\psi\rangle = 2^{-1/2}(|0, 0\rangle - i|1, 1\rangle)$. Once entanglement is achieved, the CNOT gate can be implemented with additional single particle rotations, carried out analogously to those in the Cirac–Zoller scheme, with individual laser beams exciting single ions. Simultaneous entanglement of any *even* number of ions can be carried out similarly, although the CNOT gate applied to *any pair* of ions is sufficient for computation. The technique has been experimentally demonstrated with four ions in a small linear ion trap [22].

(b) The Jonathan–Plenio scheme [15].

When an atomic transition is driven by a laser beam at resonance, an AC Stark shift (or light shift) results, changing the energies of the coupled levels due to the coupling to the laser field. The laser drive on an ion in a linear string in a trap produces Rabi transitions between the coupled levels, but if the Rabi frequency matches one of the CM vibration modes ν_p of the ion string, an exchange of excitation energy between the internal and vibrational variables also occurs. This exchange can be used to derive a CNOT gate between any two ions in the linear chain, based on an interference analogous to that of the Sørensen–Mølmer scheme discussed above. This is expected to result in relatively fast quantum gates, but requires cold ions. When the light shift is used to drive virtual two-phonon transitions simultaneously, using more than one vibrational mode, it is predicted that gate speeds will be somewhat reduced, but the ions remain insensitive to heating, possibly offering an advantage over the Sørensen–Mølmer scheme. Two ion states of the form $|1, 0\rangle|n_p\rangle$ and $|0, 1\rangle|n_p\rangle$ are coupled. The effective time-independent Hamiltonian is written $-\hbar\omega[|1, 0\rangle\langle 0, 1| + |0, 1\rangle\langle 1, 0|]$ plus a sum over states p which depend on the ion motion, but which can be cancelled by reversing the sign of a parameter half way through the operation. The states in the Hamiltonian are assumed now to be “dressed”, i.e., formed from the original states coupled and shifted by interaction with the external field. The frequency is $\omega = (\Omega^2/2)\sum_{p=1}^N\eta_{1p}\eta_{2p}\nu_p/(\Omega^2 - \nu_p^2)$. Maximally entangled states can be produced at the time $T = |\pi/4\omega|$. This proposed technique has not yet been experimentally demonstrated.

5. Quantum Dots

Quantum dots are fabricated from semiconductor materials, metals, or small molecules. They work by confining electric charge quanta (i.e., spins) in three dimensional boxes with electrostatic potentials. The spin of a charge quantum in a single quantum dot can be manipulated, i.e., single qubit operations, by applying pulsed local electromagnetic fields, through a scanning-probe tip, for example. Two-qubit operations can be achieved by spectroscopic manipulation or by a purely electrical gating of the tunneling barrier between neighboring quantum dots.

The spin-1/2 operator of an electron is given by

$$(5.1) \quad \mathbf{S} = (\sigma_x, \sigma_y, \sigma_z)^T = \sigma_x \mathbf{e}_x + \sigma_y \mathbf{e}_y + \sigma_z \mathbf{e}_z$$

where σ_x, σ_y and σ_z are the usual Pauli matrices:

$$(5.2) \quad \sigma_x = \begin{bmatrix} 0 & 1 \\ 1 & 0 \end{bmatrix}, \quad \sigma_y = \begin{bmatrix} 0 & -i \\ i & 0 \end{bmatrix}, \quad \sigma_z = \begin{bmatrix} 1 & 0 \\ 0 & -1 \end{bmatrix},$$

and

$$(5.3) \quad \mathbf{e}_x = \begin{bmatrix} 1 \\ 0 \\ 0 \end{bmatrix}, \quad \mathbf{e}_y = \begin{bmatrix} 0 \\ 1 \\ 0 \end{bmatrix}, \quad \mathbf{e}_z = \begin{bmatrix} 0 \\ 0 \\ 1 \end{bmatrix}$$

are the unit vectors in the directions of x, y and z . Let \mathbf{S}_i and \mathbf{S}_j denote, respectively, the spin of the electric charge quanta at, respectively, the i -th and j -th location of the quantum dots. Then the usual physics of the Hubbard model [1] gives the Hamiltonian of the system of n quantum dots as

$$(5.4) \quad H = \sum_{j=1}^n \mu_B g_j(t) \mathbf{B}_j(t) \cdot \mathbf{S}_j + \sum_{1 \leq j < k \leq n} J_{jk}(t) \mathbf{S}_j \cdot \mathbf{S}_k,$$

where the first summation denotes the sum of energy due to the application of a magnetic field \mathbf{B}_j to the electron spin at dot j , while the second denotes the interaction Hamiltonian through the tunneling effect of a gate voltage applied between the dots, and

$$(5.5) \quad \begin{aligned} \mu_B: & \text{ is the Bohr magneton;} \\ g_j(t): & \text{ is the effective } g\text{-factor;} \\ \mathbf{B}_j(t): & \text{ is the applied magnetic field;} \\ J_{jk}(t): & \text{ the time-dependent exchange constant [18, see [10] in the Refer-} \\ & \text{ ences therein], with } J_{jk}(t) = 4t_{jk}^2(t)/u, \text{ which is produced by the} \\ & \text{ turning on and off of the tunneling matrix element } t_{ij}(t) \text{ between} \\ & \text{ quantum dots } i \text{ and } j, \text{ with } u \text{ being the charging energy of a single} \\ & \text{ dot.} \end{aligned}$$

Note that for

$$(5.6) \quad \mathbf{S}_j = \sigma_x^{(j)} \mathbf{e}_x + \sigma_y^{(j)} \mathbf{e}_y + \sigma_z^{(j)} \mathbf{e}_z, \quad j = 1, 2, \dots, n,$$

and

$$(5.7) \quad \mathbf{B}_j(t) = b_x^{(j)}(t) \mathbf{e}_x + b_y^{(j)}(t) \mathbf{e}_y + b_z^{(j)}(t) \mathbf{e}_z, \quad j = 1, 2, \dots, n,$$

the dot products in (5.4) are defined by

$$(5.8) \quad \begin{aligned} \mathbf{S}_j \cdot \mathbf{S}_k &= \sigma_x^{(j)} \sigma_x^{(k)} + \sigma_y^{(j)} \sigma_y^{(k)} + \sigma_z^{(j)} \sigma_z^{(k)}, \\ \mathbf{B}_j(t) \cdot \mathbf{S}_j &= b_x^{(j)}(t) \sigma_x^{(j)} + b_y^{(j)}(t) \sigma_y^{(j)} + b_z^{(j)}(t) \sigma_z^{(j)}. \end{aligned}$$

In Fig. 5.1, we include a quantum dot array design given in Burkard, Engel and Loss [6].

Again, by the universal quantum computing theorems in §2, we need only discuss the case of a system with two quantum dots. The spin-up \uparrow and spin-down \downarrow of the electric charge quanta in each dot are denoted as $|0\rangle$ and $|1\rangle$, respectively. Then the underlying Hilbert space is

$$(5.9) \quad \mathcal{H} = \text{span}\{|00\rangle, |01\rangle, |10\rangle, |11\rangle\}.$$

The wave function $|\psi(t)\rangle$ of the system has four components:

$$(5.10) \quad |\psi(t)\rangle = \psi_1(t)|00\rangle + \psi_2(t)|01\rangle + \psi_3(t)|10\rangle + \psi_4(t)|11\rangle,$$

satisfying the Schrödinger equation

$$(5.11) \quad \begin{cases} i\hbar \frac{\partial}{\partial t} |\psi(t)\rangle = H(t) |\psi(t)\rangle, & t > 0, \\ |\psi(0)\rangle = |\psi_0\rangle \in \mathcal{H}, \end{cases}$$

where

$$(5.12) \quad H(t) \equiv \frac{\hbar}{2} [\mathbf{\Omega}_1(t) \cdot \boldsymbol{\sigma} + \mathbf{\Omega}_2(t) \cdot \boldsymbol{\tau} + \omega(t) \boldsymbol{\sigma} \cdot \boldsymbol{\tau}],$$

following from (5.4) by rewriting the notation

$$(5.13) \quad \mathbf{S}_1 = \boldsymbol{\sigma}, \quad \mathbf{S}_2 = \boldsymbol{\tau}; \quad \mu_B g_j(t) \mathbf{B}_j(t) = \frac{\hbar}{2} \mathbf{\Omega}_j(t), \quad j = 1, 2; \quad J_{12}(t) = \frac{\hbar}{2} \omega(t).$$

The $\mathbf{\Omega}_1(t), \mathbf{\Omega}_2(t)$ and $\omega(t)$ in (5.12) are the *control pulses*.

Let us now give a brief heuristic physics discussion for the derivation of the Hamiltonian in (5.4) and (5.12) as a remark below.

REMARK 5.1. The suggestion to use quantum dots as qubits for the purposes of quantum information processing in general, and quantum computing in particular, is based on the following observations. To set the stage, we note that a quantum dot is formed by a single electron that is tightly bound to a “center” – some distinguished small area in a solid. Typically, the binding is strongly confining in one spatial direction (the z direction) while the electron has some freedom of motion in the plane perpendicular to it (the xy plane), with its dynamics governed by the forces that bind it to its center. In addition, there is the possibility of applying electric and magnetic fields of varying strength and direction, whereby the experimenter can exert some external control over the evolution of the electron’s state.

In particular, a magnetic field $\mathbf{B}(t)$ will couple to the magnetic moment of the electron, which gives rise to a term in the Hamilton operator that is proportional to $\mathbf{B} \cdot \boldsymbol{\sigma}$, where $\boldsymbol{\sigma}$ is the Pauli spin vector operator of the electron, so that

$$(5.14) \quad H = \frac{1}{2} \hbar \mathbf{\Omega}(t) \cdot \boldsymbol{\sigma}$$

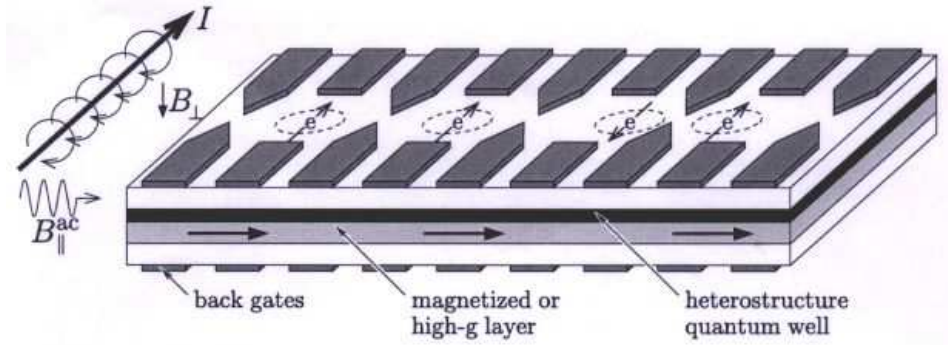


FIGURE 5.1. Quantum dot array, controlled by electrical gating. The electrodes (dark gray) define quantum dots (circles) by confining electrons. The spin 1/2 ground state (arrow) of the dot represents the qubit. These electrons can be moved by electrical gating into the magnetized or high- g layer, producing locally different Zeeman splittings. Alternatively, magnetic field gradients can be applied, as e.g. produced by a current wire (indicated on the left of the dot-array). Then, since every dot-spin is subjected to a different Zeeman splitting, the spins can be addressed individually, e.g. through ESR (electron spin resonance) pulses of an additional in-plane magnetic ac field with the corresponding Larmor frequency $\omega_L = q\mu_B B_{\perp}/\hbar$. (In the figure, B_{\perp} denotes the component of the magnetic field perpendicular to the array plane, while B_{\parallel} denotes that parallel to the plane.) Such mechanisms can be used for single-spin rotations and the initialization step. The exchange coupling between the quantum dots can be controlled by lowering the tunnel barrier between the dots. In this figure, the two rightmost dots are drawn schematically as tunnel-coupled. Such an exchange mechanism can be used for the CNOT-gate operation involving two nearest neighbor qubits. The CNOT operator between distant qubits is achieved by swapping (via exchange) the qubits first to a nearest neighbor position. The read-out of the spin state can be achieved via spin-dependent tunneling and SET devices [18], or via a transport current passing the dot [18]. Note that all spin operations, single and two spin operations, and spin read-out, are controlled electrically via the charge of the electron and not via the magnetic moment of the spin. Thus, no control of local magnetic fields is required, and the spin is only used for storing the information. This spin-to-charge conversion is based on the Pauli principle and Coulomb interaction and allows for very fast switching times (typically picoseconds). A further advantage of this scheme is its scalability into an array of arbitrary size. (The figure is excerpted from Burkard, Engel and Loss [6], courtesy of Springer-Verlag Berlin Heidelberg, while the caption is excerpted from Schliemann and Loss [23].)

is the structure of the effective single-qubit Hamilton operator, with $\Omega(t) \propto \mathbf{B}(t)$ being externally controlled by the experimenter. By suitably choosing $\mathbf{B}(t)$ various single-qubit gates can be realized.

To suppress the unwanted effect of the Lorentz force (which couples to the electron's charge, results in a time-dependent energy, and thus produces an accumulated phase change), it is expedient to have the magnetic field vector in the xy plane, so that $\mathbf{B} \cdot \mathbf{e}_z = 0$ is imposed. Nevertheless, general single qubit gates can be realized by a succession of rotations of σ about axes in the xy plane. This is just an application of Euler's classical result that general rotations can be composed of successive rotations about two orthogonal axes only (standard choice is the z axis and the x axis but, of course, the x axis and the y axis serve this purpose just as well).

More complicated is the implementation of two-qubit gates. Here one needs two quantum dots in close proximity, by which is meant that they have a considerable interaction, predominantly originating in the Coulomb repulsion of the charges of the two electrons. It is important that external electric fields can be used to modify the effective interaction strength in a wide range, and in particular one can "turn it off" by separating the two quantum dots (or rather shielding them from each other).

Consider, thus, two quantum dots with some interaction potential in addition to the potentials that bind them to their respective centers. This situation is reminiscent of the hydrogen dimer, the H_2 molecule, except that the confinement to a plane and the form of the binding potential, and also of the effective interaction, are quite different. It is, indeed, not so simple to model the various potentials reasonably well, and one must be practiced in the art of solid-state theory to do it well. We shall, therefore, refer the interested reader to the specialized literature, perhaps starting with [5] and the references therein.

The general picture, however, can be grasped without getting involved with such details. First, we note that at sufficiently low temperatures, only the ground state and the first excited state of the interacting two-dot system will be dynamically relevant, at least as long as we carefully avoid exciting other states. For symmetry reasons, the ground state is a spin-singlet (total spin angular momentum of $0\hbar$) and has a symmetric spatial wave function, whereas the first excited state is a spin-triplet (total spin angular momentum of $1\hbar$) and has an antisymmetric spatial wave function. The excited state is long-lived because triplet-to-singlet transitions tend to have very small matrix elements.

The total spin angular momentum vector operator is $\mathbf{S} = \frac{1}{2}\hbar(\boldsymbol{\sigma} + \boldsymbol{\tau})$ where we denote the Pauli vector operators of the two electrons by $\boldsymbol{\sigma}$ and $\boldsymbol{\tau}$, respectively. The eigenvalues of \mathbf{S}^2 are $0\hbar^2$ in the spin singlet and $2\hbar^2$ in the spin triplet. In view of $\boldsymbol{\sigma}^2 = 3\mathbf{1}$ and $\boldsymbol{\tau}^2 = 3\mathbf{1}$, this says that $\boldsymbol{\sigma} \cdot \boldsymbol{\tau}$ has eigenvalue -3 in the singlet and $+1$ in the triplet. As a consequence,

$$(5.15) \quad \begin{cases} \frac{1}{4}(\mathbf{1} - \boldsymbol{\sigma} \cdot \boldsymbol{\tau}) \text{ projects on the singlet, and} \\ \frac{1}{4}(\mathbf{3}\mathbf{1} + \boldsymbol{\sigma} \cdot \boldsymbol{\tau}) \text{ projects on the triplet.} \end{cases}$$

Effectively, then, they project on the ground state and the excited state, respectively. Denoting by E_0 the ground state energy, and by $E_1 = E_0 + 2\hbar\omega$ that of the

excited state, we have

$$\begin{aligned}
 H &= \frac{1}{4}(\mathbf{1} - \boldsymbol{\sigma} \cdot \boldsymbol{\tau})E_0 + \frac{1}{4}(3\mathbf{1} + \boldsymbol{\sigma} \cdot \boldsymbol{\tau})E_1 \\
 &= \frac{1}{4}(E_0 + 3E_1)\mathbf{1} + \frac{1}{4}(E_1 - E_0)\boldsymbol{\sigma} \cdot \boldsymbol{\tau}
 \end{aligned}
 \tag{5.16}$$

or, after dropping the irrelevant additive constant,

$$H = \frac{1}{2}\hbar\omega(t)\boldsymbol{\sigma} \cdot \boldsymbol{\tau}
 \tag{5.17}$$

for the effective Hamilton operator of the coupling between the two quantum dots. We have indicated the externally controlled time dependence of ω , the “turning on” and “turning off” of the interaction at the experimenter’s discretion, by t .

In summary, then, we have two terms of the form (5.14), one for each quantum dot, and the interaction term (5.17) in the effective Hamilton operator

$$H = \frac{1}{2}\hbar[\boldsymbol{\Omega}_1(t) \cdot \boldsymbol{\sigma} + \boldsymbol{\Omega}_2(t) \cdot \boldsymbol{\tau} + \omega(t)\boldsymbol{\sigma} \cdot \boldsymbol{\tau}].
 \tag{5.18}$$

Within reasonable ranges, the experimenter is capable of realizing any $\boldsymbol{\Omega}_1(t)$, $\boldsymbol{\Omega}_2(t)$, and $\omega(t)$, where it is fully sufficient to have two of them vanishing at any instant. \square

LEMMA 5.1. *Let $\boldsymbol{\sigma}$ and $\boldsymbol{\tau}$ be defined as in (5.13). Then we have*

$$\text{(i) } \left(\frac{1 + \boldsymbol{\sigma} \cdot \boldsymbol{\tau}}{2}\right)^2 = \mathbf{1} \text{ and } (\boldsymbol{\sigma} \cdot \boldsymbol{\tau})^2 = 3\mathbf{1} - 2\boldsymbol{\sigma} \cdot \boldsymbol{\tau}.
 \tag{5.19}$$

$$\text{(ii) } U_{\text{sw}} = \frac{1}{2}(\mathbf{1} + \boldsymbol{\sigma} \cdot \boldsymbol{\tau}) = U_{\text{sw}}^\dagger = U_{\text{sw}}^{-1}, \text{ where } U_{\text{sw}} \text{ is the swapping gate}
 \tag{5.20}$$

$$U_{\text{sw}}|jk\rangle = |kj\rangle \quad \text{for } j, k = 0, 1; \text{ cf. (2.14)}.
 \tag{5.21}$$

(iii)

$$U_{\text{sw}}^\dagger \boldsymbol{\sigma} U_{\text{sw}} = \boldsymbol{\tau}, \quad U_{\text{sw}}^\dagger \boldsymbol{\tau} U_{\text{sw}} = \boldsymbol{\sigma}
 \tag{5.22}$$

$$\text{(iv) } U_{\text{sw}}^2 = \mathbf{1}.
 \tag{5.23}$$

PROOF. Let us recall first how the various σ_j and τ_j transform the basis vectors, for $j = x, y, z$:

$$\begin{aligned}
 \sigma_x|0\cdot\rangle &= |1\cdot\rangle, & \sigma_x|1\cdot\rangle &= |0\cdot\rangle, \\
 \sigma_y|0\cdot\rangle &= i|1\cdot\rangle, & \sigma_y|1\cdot\rangle &= -i|0\cdot\rangle, \\
 \sigma_z|0\cdot\rangle &= |0\cdot\rangle, & \sigma_z|1\cdot\rangle &= -|1\cdot\rangle,
 \end{aligned}
 \tag{5.24}$$

and likewise for τ_x , τ_y , and τ_z acting on $|\cdot 0\rangle$ and $|\cdot 1\rangle$. Thus

$$\begin{aligned}
 \boldsymbol{\sigma} \cdot \boldsymbol{\tau}|00\rangle &= (1^2 + i^2)|11\rangle + |00\rangle = |00\rangle, \\
 \boldsymbol{\sigma} \cdot \boldsymbol{\tau}|01\rangle &= (1^2 - i^2)|10\rangle - |01\rangle = 2|10\rangle - |01\rangle, \\
 \boldsymbol{\sigma} \cdot \boldsymbol{\tau}|10\rangle &= (1^2 - i^2)|01\rangle + |10\rangle = 2|01\rangle - |10\rangle, \\
 \boldsymbol{\sigma} \cdot \boldsymbol{\tau}|11\rangle &= (1^2 + i^2)|00\rangle + |11\rangle = |11\rangle,
 \end{aligned}
 \tag{5.25}$$

and we see that the 4×4 matrix for $\boldsymbol{\sigma} \cdot \boldsymbol{\tau}$ is given by

$$(5.26) \quad \boldsymbol{\sigma} \cdot \boldsymbol{\tau} = \begin{bmatrix} 1 & 0 & 0 & 0 \\ 0 & -1 & 2 & 0 \\ 0 & 2 & -1 & 0 \\ 0 & 0 & 0 & 1 \end{bmatrix},$$

and the first equation in (5.19) follows.

We read off that $\boldsymbol{\sigma} \cdot \boldsymbol{\tau}$ has a 3-fold eigenvalue $+1$ and a single eigenvalue -3 . The respective projectors to the subspaces characterized by these eigenvalues are easily verified to be

$$(5.27) \quad \mathbb{P}_1 \equiv \frac{1}{4}(\mathbf{31} + \boldsymbol{\sigma} \cdot \boldsymbol{\tau}) \quad \text{and} \quad \mathbb{P}_2 \equiv \frac{1}{4}(\mathbf{1} - \boldsymbol{\sigma} \cdot \boldsymbol{\tau}),$$

where $\mathbb{P}_j^2 = \mathbb{P}_j$ for $j = 1, 2$, and $\mathbb{P}_j \mathbb{P}_k = 0$ for $j \neq k$. Therefore, for any sufficiently well-behaved function, including polynomials and analytic functions, of $\boldsymbol{\sigma} \cdot \boldsymbol{\tau}$,

$$(5.28) \quad \begin{aligned} f(\boldsymbol{\sigma} \cdot \boldsymbol{\tau}) &= f(1) \frac{1}{4}(\mathbf{31} + \boldsymbol{\sigma} \cdot \boldsymbol{\tau}) + f(-3) \frac{1}{4}(\mathbf{1} - \boldsymbol{\sigma} \cdot \boldsymbol{\tau}) \\ &= \frac{1}{4}[3f(1) + f(-3)]\mathbf{1} + \frac{1}{4}[f(1) - f(-3)]\boldsymbol{\sigma} \cdot \boldsymbol{\tau}, \end{aligned}$$

according to the spectral theorem. As a first application, consider $f(x) = x^2$ and find

$$(5.29) \quad (\boldsymbol{\sigma} \cdot \boldsymbol{\tau})^2 = \mathbf{31} - 2\boldsymbol{\sigma} \cdot \boldsymbol{\tau},$$

which is the second equation in (5.19).

Further, in view of the matrix for U_{sw} ,

$$(5.30) \quad U_{\text{sw}} = \frac{1}{2}(\mathbf{1} + \boldsymbol{\sigma} \cdot \boldsymbol{\tau}) = \begin{bmatrix} 1 & 0 & 0 & 0 \\ 0 & 0 & 1 & 0 \\ 0 & 1 & 0 & 0 \\ 0 & 0 & 0 & 1 \end{bmatrix}$$

the swapping gate really swaps: $U_{\text{sw}}|jk\rangle = |kj\rangle$ (no effect on $|00\rangle$ and $|11\rangle$, whereas $|01\rangle$ and $|10\rangle$ are interchanged). To verify

$$(5.31) \quad U_{\text{sw}}\boldsymbol{\sigma} = \boldsymbol{\tau}U_{\text{sw}}$$

it should suffice to inspect the pair

$$(5.32) \quad \sigma_x = |00\rangle\langle 10| + |01\rangle\langle 11| + |10\rangle\langle 00| + |11\rangle\langle 01|$$

and

$$(5.33) \quad \tau_x = |00\rangle\langle 01| + |10\rangle\langle 11| + |01\rangle\langle 00| + |11\rangle\langle 10|,$$

for example. One can also have a purely algebraic, but more lengthy, argument that exploits nothing but the basic identities, such as $\sigma_x^2 = \mathbf{1}$ and $\sigma_1\sigma_2 = i\sigma_3$, etc. Thus, the rest easily follows. \square

THEOREM 5.2. *Denote by $U(t)$ the time evolution operator for the quantum system (5.11) and (5.12) for time duration $t \in [0, T]$. Choose $\boldsymbol{\Omega}_1(t) = \boldsymbol{\Omega}_2(t) = 0$ in (5.12) and let $\omega(t)$ therein satisfies*

$$(5.34) \quad \int_0^T \omega(t)dt = \frac{\pi}{2}.$$

Then we have $U(T) = -e^{\pi i/4}U_{\text{sw}}$, i.e., $U(T)$ is the swapping gate (with a nonessential phase factor $-e^{\pi i/4}$.)

PROOF. By assumptions, we have now

$$(5.35) \quad H(t) = \omega(t)\boldsymbol{\sigma} \cdot \boldsymbol{\tau}/2.$$

Since $\omega(t)$ is scalar-valued, we have the commutativity

$$(5.36) \quad H(t_1)H(t_2) = H(t_2)H(t_1), \quad \text{for any } t_1, t_2 \in [0, T].$$

Therefore

$$(5.37) \quad \begin{aligned} U(T) &= e^{-i \int_0^T H(t) dt / \hbar} = e^{[-\frac{i}{2} \int_0^T \omega(t) dt] \boldsymbol{\sigma} \cdot \boldsymbol{\tau}} \\ &= e^{-i\phi \boldsymbol{\sigma} \cdot \boldsymbol{\tau}} \quad \left(\phi \equiv \frac{1}{2} \int_0^T \omega(t) dt \right) \\ &= \cos(\phi \boldsymbol{\sigma} \cdot \boldsymbol{\tau}) - i \sin(\phi \boldsymbol{\sigma} \cdot \boldsymbol{\tau}), \end{aligned}$$

where $e^{-i\phi \boldsymbol{\sigma} \cdot \boldsymbol{\tau}}$, $\cos(\phi \boldsymbol{\sigma} \cdot \boldsymbol{\tau})$ and $\sin(\phi \boldsymbol{\sigma} \cdot \boldsymbol{\tau})$ are 4×4 matrices. We now utilize (5.28) to calculate the exponential matrix $U(T)$:

$$(5.38) \quad U(T) = e^{-i\phi \boldsymbol{\sigma} \cdot \boldsymbol{\tau}} = e^{-i\phi} \cdot \frac{1}{4}(3\mathbf{1} + \boldsymbol{\sigma} \cdot \boldsymbol{\tau}) + e^{-3i\phi} \cdot \frac{1}{4}(\mathbf{1} - \boldsymbol{\sigma} \cdot \boldsymbol{\tau}).$$

Thus, with a little manipulation, (5.38) becomes

$$(5.39) \quad \begin{aligned} U(T) &= e^{i\phi} \left[\cos(2\phi)\mathbf{1} - i \sin(2\phi) \frac{\mathbf{1} + \boldsymbol{\sigma} \cdot \boldsymbol{\tau}}{2} \right] \\ &= e^{i\phi} [\cos(2\phi)\mathbf{1} - i \sin(2\phi)U_{\text{sw}}], \quad \text{by (5.20).} \end{aligned}$$

Choosing $\phi = \pi/4$, we obtain the desired conclusion. \square

COROLLARY 5.3. The square roots of the swapping gate, $U_{\text{sw}}^{1/2}$, are

$$(5.40) \quad U_{\text{sw}}^{1/2} = \frac{e^{\pm \pi i/4}}{\sqrt{2}}(\mathbf{1} \mp iU_{\text{sw}}).$$

PROOF. From (5.39), we first obtain

$$(5.41) \quad U_{\text{sw}} = ie^{-\frac{\pi i}{4}}U(T).$$

Then use $\phi = \pm\pi/8$ in (5.39) to obtain

$$(5.42) \quad U_{\text{sw}}^{1/2} = (ie^{-\frac{\pi i}{4}})^{1/2} e^{\pm \pi i/8} \left[\frac{1}{\sqrt{2}}(\mathbf{1} \mp iU_{\text{sw}}) \right]$$

and the desired conclusion. (Note that these two square roots of U_{sw} reflect the choices of $\sqrt{\mathbf{1}} = 1$ and

$$(5.43) \quad \text{the square root of } -1 = \pm i$$

for the square roots of the eigenvalues of U_{sw} .) \square

Theorem 5.2 gives us the choice of control pulses $\omega(t)$ (with $\boldsymbol{\Omega}_1(t)$ and $\boldsymbol{\Omega}_2(t)$ being set to 0) which yields the swapping gate U_{sw} , which does not cause entanglement. However, $U_{\text{sw}}^{1/2}$ in Corollary 5.3 causes entanglement. See Corollary 5.5 shortly.

THEOREM 5.4. *Let $\phi, \theta \in [0, 2\pi]$ be given. Denote $\mathbf{e}(\phi) = \cos \phi \mathbf{e}_x + \sin \phi \mathbf{e}_y + 0\mathbf{e}_z$ for the given ϕ . Let $U_{1,\mathbf{\Omega}_1}(t)$ be the time evolution operator corresponding to the quantum system (5.11) and (5.12) for $t \in [0, T]$ where the pulses are chosen such that*

$$(5.44) \quad \mathbf{\Omega}_1(t) = \Omega_1(t)\mathbf{e}(\phi), \quad \mathbf{\Omega}_2(t) = 0, \quad \omega(t) = 0, \quad t \in [0, T],$$

with $\Omega_1(t)$ satisfying

$$(5.45) \quad \int_0^T \Omega_1(t) dt = 2\theta, \quad \text{for the given } \theta.$$

Then the action of $U_{1,\mathbf{\Omega}_1}(t)$ on the first qubit satisfies

$$(5.46) \quad U_{1,\mathbf{\Omega}_1}(t) = U_{\theta,\phi}, \quad \text{the 1-bit unitary rotation gate (2.17).}$$

PROOF. We have

$$\begin{aligned} U_{\theta,\phi} &= \begin{bmatrix} \cos \theta & -ie^{-i\phi} \sin \theta \\ -ie^{i\phi} \sin \theta & \cos \theta \end{bmatrix} \\ &= \cos \theta \mathbf{1} - ie^{-i\phi} \sin \theta \left(\frac{\sigma_x - i\sigma_y}{2} \right) - ie^{i\phi} \sin \theta \left(\frac{\sigma_x + i\sigma_y}{2} \right) \\ &= \cos \theta \mathbf{1} - i \sin \theta \cos \phi \sigma_x - i \sin \theta \sin \phi \sigma_y \\ &= \cos \theta \mathbf{1} - i \sin \theta (\cos \phi \sigma_x + \sin \phi \sigma_y) \\ &= \cos \theta \mathbf{1} - i \sin \theta \mathbf{e}(\phi) \cdot \boldsymbol{\sigma} \\ (5.47) \quad &= e^{-i\theta \mathbf{e}(\phi) \cdot \boldsymbol{\sigma}}, \end{aligned}$$

noting that in the above, we have utilized the fact that the 2×2 matrix

$$(5.48) \quad \mathbf{e}(\phi) \cdot \boldsymbol{\sigma} = \begin{bmatrix} 0 & \cos \phi - i \sin \phi \\ \cos \phi + i \sin \phi & 0 \end{bmatrix}$$

satisfies $(\mathbf{e}(\phi) \cdot \boldsymbol{\sigma})^{2n} = \mathbf{1}$ for $n = 0, 1, 2, \dots$.

With the choices of the pulses as given in (5.44), we see that the second qubit remains steady in the time-evolution of the system. The Hamiltonian, now, is

$$(5.49) \quad H_1(t) = \frac{\hbar}{2} \Omega_1(t) \mathbf{e}_1(\phi) \cdot \boldsymbol{\sigma}$$

and acts only on the first qubit (where the subscript 1 of $\mathbf{e}_1(\phi)$ denotes that this is the vector $\mathbf{e}(\phi)$ for the first bit). Because $\Omega_1(t)$ is scalar-valued, we have

$$(5.50) \quad H_1(t_1)H_1(t_2) = H_1(t_2)H_1(t_1) \quad \text{for any } t_1, t_2 \in [0, T].$$

Thus

$$\begin{aligned} U_{1,\mathbf{\Omega}_1}(T) &= e^{-\frac{i}{\hbar} \int_0^T \Omega_1(t) \mathbf{e}_1(\phi) \cdot \boldsymbol{\sigma} dt} \\ &= e^{-\frac{i}{\hbar} \int_0^T \Omega_1(t) dt} \mathbf{e}_1(\phi) \cdot \boldsymbol{\sigma} \\ (5.51) \quad &= e^{-i\theta \mathbf{e}_1(\phi) \cdot \boldsymbol{\sigma}}, \quad (\text{by (5.45)}) \end{aligned}$$

using (5.47). The proof is complete. \square

We may define $U_{2,\mathbf{\Omega}_2}$ in a similar way as in Theorem 5.4.

COROLLARY 5.5. *The quantum phase gate Q_π (2.18) is given by*

$$(5.52) \quad Q_\pi = (-i)U_{1,\Omega_1^{(2)}}U_{2,\Omega_2}U_{\text{sw}}^{1/2}U_{1,\Omega_1^{(1)}}U_{\text{sw}}^{1/2},$$

where

$$(5.53) \quad \begin{cases} \int \Omega_1^{(1)}(t) dt = -\pi \mathbf{e}_{1z}, \\ \int \Omega_1^{(2)}(t) dt = \pi \mathbf{e}_{1z}/2, \\ \int \Omega_2(t) dt = -\pi \mathbf{e}_{2z}/2, \end{cases}$$

and $\mathbf{e}_{1z}, \mathbf{e}_{2z}$ denote the \mathbf{e}_z vector of, respectively, the first and the second qubit.

REMARK 5.2. In order to realize this succession of gates, only one of the $\Omega(t)$ in (5.53) is nonzero at any given instant t , with the duration when $\Omega_1^{(1)}(t) \neq 0$ earlier than that when $\Omega_2(t) \neq 0$, and that when $\Omega_1^{(2)}(t) \neq 0$ even later. Earliest is the period when $\omega(t) \neq 0$ for the first $U_{\text{sw}}^{1/2}$, and another period when $\omega(t) \neq 0$ is intermediate between those when $\Omega_1^{(1)}(t) \neq 0$ and $\Omega_2(t) \neq 0$.

PROOF. Define

$$(5.54) \quad U_{\text{XOR}} \equiv e^{\frac{\pi i}{4}\sigma_z} e^{-\frac{\pi i}{4}\tau_z} U_{\text{sw}}^{1/2} e^{i\frac{\pi}{2}\sigma_z} U_{\text{sw}}^{1/2},$$

with $U_{\text{sw}}^{1/2} = \frac{e^{-\frac{\pi}{4}i}}{\sqrt{2}}(\mathbf{1} + iU_{\text{sw}})$ chosen from (5.40). Then it is straightforward to check that

$$(5.55) \quad \begin{aligned} U_{\text{XOR}}|00\rangle &= |00\rangle(i), & U_{\text{XOR}}|01\rangle &= |01\rangle(i), \\ U_{\text{XOR}}|10\rangle &= |10\rangle(i), & U_{\text{XOR}}|11\rangle &= |11\rangle(-i), \end{aligned}$$

so that

$$(5.56) \quad \begin{aligned} U_{\text{XOR}} &= i(|00\rangle\langle 00| + |01\rangle\langle 01| + |10\rangle\langle 10| - |11\rangle\langle 11|) \\ &= iQ_\pi. \end{aligned}$$

□

REMARK 5.3. In [18, eq. (2)], Loss and DiVincenzo write their U_{XOR} gate as

$$(5.57) \quad U_{\text{XOR}} = e^{i\frac{\pi}{2}S_1^z} e^{-i\frac{\pi}{2}S_2^z} U_{\text{sw}}^{1/2} e^{i\pi S_1^z} U_{\text{sw}}^{1/2}.$$

Thus there is a difference in notation between the above and (5.54):

$$(5.58) \quad S_1^2 = \sigma_z/2, \quad S_2^z = \tau_z/2.$$

□

THEOREM 5.6. *The quantum computer made of quantum dots is universal.*

PROOF. This follows easily from (2.19), Theorem 5.4, Corollary 5.5, and finally Corollary 2.3. □

Throughout this paper we have been employing the Schrödinger point of view and could therefore afford to identify the ket vectors with particular numerical column vectors, the bra vectors with the corresponding row vectors, and we did not distinguish between operators and matrices. Now, let us give a brief, heuristic exposition from the point of view of the Heisenberg picture, in which it is important to discriminate between kets and their columns, bras and their rows, operators and their matrices. Dirac's classic text [11] and the recent textbook by Schwinger [24] treat quantum mechanics consistently in the Heisenberg picture.

For a start we return to (5.9) and (5.10) where each $|jk\rangle$ is a joint eigenket of σ_z and τ_z with eigenvalues $1 - 2j$ and $1 - 2k$, respectively for $j, k = 0, 1$. A simultaneous measurement of σ_z and τ_z yields the actual one of the four pairs of values and tells us which of the four possibilities is the case.

Now, a measurement of σ_z , say, at time t_1 is not the same as a measurement of σ_z at time t_2 , one really has to perform two different experiments (perhaps using the same lab equipment twice). Therefore, according to the reasoning of Heisenberg and Dirac, just to mention the main quantum physicists, we should also have two mathematical symbols for these two measurements: $\sigma_z(t_1)$ and $\sigma_z(t_2)$. As a consequence, then, also the eigenkets must refer to the time of measurement: $|jk, t_1\rangle$ and $|jk, t_2\rangle$. Accordingly, the eigenvector equations read

$$(5.59) \quad \left. \begin{aligned} \sigma_z(t)|jk, t\rangle &= |jk, t\rangle(1 - 2j) \\ \tau_z(t)|jk, t\rangle &= |jk, t\rangle(1 - 2k) \end{aligned} \right\} \text{ for all } t, \text{ for } j, k = 0, 1.$$

On the other hand, the state of the system, which is typically specified by a statement of the kind “at time t_0 both spins were up in the z direction” (formally: state ket $|\Psi\rangle = |00, t_0\rangle$), does not depend on time by its nature. So, rather than (5.10), we write

$$(5.60) \quad |\Psi\rangle = \psi_1(t)|00, t\rangle + \psi_2(t)|01, t\rangle + \psi_3(t)|10, t\rangle + \psi_4(t)|11, t\rangle,$$

where the *dynamical* time dependences of the kets $|00, t\rangle, \dots, |11, t\rangle$ is compensated for by the *parametric* time dependence of the probability amplitudes $\psi_1(t), \dots, \psi_4(t)$, so that the state ket $|\Psi\rangle$ is constant in time, as it should be.

The probability amplitudes are thus given by

$$(5.61) \quad \psi_1(t) = \langle 00, t | \Psi \rangle, \quad \psi_2(t) = \langle 01, t | \Psi \rangle, \quad \psi_3(t) = \langle 10, t | \Psi \rangle, \quad \psi_4(t) = \langle 11, t | \Psi \rangle,$$

and they have the same meaning as before: $|\psi_2(t)|^2$, for example, is the probability that the first spin is found up and the second down at time t . And, of course, they obey the same Schrödinger equation as before, namely (5.11) where $|\psi(t)\rangle$ is just the column $[\psi_1(t) \ \psi_2(t) \ \psi_3(t) \ \psi_4(t)]^T$ and $H(t)$ the 4×4 matrix that is meant in (5.12).

With the Hamilton *operator* (not matrix!)

$$(5.62) \quad H(\boldsymbol{\sigma}(t), \boldsymbol{\tau}(t), t) = \frac{\hbar}{2} [\boldsymbol{\Omega}_1(t) \cdot \boldsymbol{\sigma}(t) + \boldsymbol{\Omega}_2(t) \cdot \boldsymbol{\tau}(t) + \omega(t) \boldsymbol{\sigma}(t) \cdot \boldsymbol{\tau}(t)],$$

which has a dynamical time dependence in $\boldsymbol{\sigma}(t)$ and $\boldsymbol{\tau}(t)$ and a parametric time dependence in $\boldsymbol{\Omega}_j(t)$, $j = 1, 2$, and $\omega(t)$, the four rows of this Schrödinger equation are just

$$(5.63) \quad i\hbar \frac{\partial}{\partial t} \langle jk, t | \Psi \rangle = \langle jk, t | H(\boldsymbol{\sigma}(t), \boldsymbol{\tau}(t), t) | \Psi \rangle \quad \text{for } jk = 00, 01, 10, 11$$

and the elements of the 4×4 matrix of (5.12) are

$$(5.64) \quad \langle jk, t | H(\boldsymbol{\sigma}(t), \boldsymbol{\tau}(t), t) | lm, t \rangle \quad \text{with } jk = 00, 01, 10, 11 \text{ and } lm = 00, 01, 10, 11.$$

The Pauli matrices in (5.2) appear when we express the components of $\boldsymbol{\sigma}(t)$ explicitly in terms of the eigenkets and eigenbras of $\sigma_z(t)$ and $\tau_z(t)$,

$$(5.65) \quad \begin{aligned} \sigma_x(t) &= \sum_{k=0,1} (|0k, t\rangle \langle 1k, t| + |1k, t\rangle \langle 0k, t|) \\ &= \sum_{k=0,1} \begin{bmatrix} |0k, t\rangle \\ |1k, t\rangle \end{bmatrix} \begin{bmatrix} 0 & 1 \\ 1 & 0 \end{bmatrix} [\langle 0k, t|, \langle 1k, t|], \\ \sigma_y(t) &= \sum_{k=0,1} \begin{bmatrix} |0k, t\rangle \\ |1k, t\rangle \end{bmatrix} \begin{bmatrix} 0 & -i \\ i & 0 \end{bmatrix} [\langle 0k, t|, \langle 1k, t|], \\ \sigma_z(t) &= \sum_{k=0,1} \begin{bmatrix} |0k, t\rangle \\ |1k, t\rangle \end{bmatrix} \begin{bmatrix} 1 & 0 \\ 0 & -1 \end{bmatrix} [\langle 0k, t|, \langle 1k, t|], \end{aligned}$$

and likewise for $\boldsymbol{\tau}(t)$, compactly written as

$$(5.66) \quad \boldsymbol{\tau}(t) = \sum_{j=0,1} \begin{bmatrix} |j0, t\rangle \\ |j1, t\rangle \end{bmatrix} \left(\begin{bmatrix} 0 & 1 \\ 1 & 0 \end{bmatrix} \mathbf{e}_x + \begin{bmatrix} 0 & -i \\ i & 0 \end{bmatrix} \mathbf{e}_y + \begin{bmatrix} 1 & 0 \\ 0 & -1 \end{bmatrix} \mathbf{e}_z \right) [\langle j0, t|, \langle j1, t|].$$

Note how numerical 2×2 matrices are sandwiched by 2-component columns of kets and 2-component rows of bras to form linear combinations of products of the dyadic ket-times-bra type.

The Schrödinger equation (5.63) is the equation of motion of the bras $\langle jk, t|$ and those of the kets $|jk, t\rangle$ is the adjoint system. The equation of motion for the operator $\boldsymbol{\sigma}(t)$ follows from them,

$$(5.67) \quad i\hbar \frac{d}{dt} \boldsymbol{\sigma}(t) = \boldsymbol{\sigma}(t) H_t - H_t \boldsymbol{\sigma}(t) = [\boldsymbol{\sigma}(t), H_t],$$

and likewise for $\boldsymbol{\tau}(t)$,

$$(5.68) \quad i\hbar \frac{d}{dt} \boldsymbol{\tau}(t) = [\boldsymbol{\tau}(t), H_t],$$

where H_t abbreviates $H(\boldsymbol{\sigma}(t), \boldsymbol{\tau}(t), t)$, the Hamilton operator of (5.62). These are particular examples of the more general *Heisenberg equation of motion*, which states that any operator – here: any function O_t of $\boldsymbol{\sigma}(t)$, $\boldsymbol{\tau}(t)$, and t itself – obeys

$$(5.69) \quad \frac{d}{dt} O_t = \frac{\partial}{\partial t} O_t + \frac{1}{i\hbar} [O_t, H_t],$$

where $\frac{d}{dt}$ is the total time derivative whereas $\frac{\partial}{\partial t}$ differentiates only the parametric time derivative, so that the commutator term accounts for the dynamical change in time of O_t . Note that (5.69) has exactly the same structure as the Hamilton equation of motion in classical mechanics.

A particular O_t is the unitary evolution operator $U_{t_0, t} \equiv U(t_0; \boldsymbol{\sigma}(t), \boldsymbol{\tau}(t), t)$ that transforms a bra at time t_0 into the corresponding bra at time t (earlier or later),

$$(5.70) \quad \langle \dots, t | = \langle \dots, t_0 | U_{t_0, t},$$

where the ellipsis stands for any corresponding set of quantum numbers (such as $00, \dots, 11$). $U_{t_0,t}$ has a parametric dependence on both t_0 and t , in addition to the dynamical t dependence that originates in $\boldsymbol{\sigma}(t)$ and $\boldsymbol{\tau}(t)$. The group property $U_{t_0,t_1}U_{t_1,t_2} = U_{t_0,t_2}$ follows from the definition and so does the unitarity, and thus

$$(5.71) \quad U_{t_0,t}^\dagger = U_{t_0,t}^{-1} = U_{t,t_0}$$

is implied immediately. Accordingly, we have

$$(5.72) \quad \boldsymbol{\sigma}(t) = U_{t,t_0}\boldsymbol{\sigma}(t_0)U_{t_0,t}, \quad \boldsymbol{\tau}(t) = U_{t,t_0}\boldsymbol{\tau}(t_0)U_{t_0,t},$$

and therefore $U(t_0; \boldsymbol{\sigma}(t), \boldsymbol{\tau}(t), t) = U(t_0; \boldsymbol{\sigma}(t_0), \boldsymbol{\tau}(t_0), t)$, that is to say: it doesn't matter if we regard U_{t,t_0} as a function of the spin operators at the initial or the final time.

Upon combining (5.70) with the Schrödinger equation (5.63), we find first

$$(5.73) \quad i\hbar \frac{d}{dt} U_{t_0,t} = U_{t_0,t} H_t,$$

and then with Heisenberg's general equation of motion (5.69),

$$(5.74) \quad i\hbar \frac{\partial}{\partial t} U_{t_0,t} = H_t U_{t_0,t}.$$

To begin with the implicit $\boldsymbol{\sigma}$ and $\boldsymbol{\tau}$ are all at time t , but since the derivative in (5.74) refers to the parametric dependence on t , not to the dynamical one, we can just as well take all $\boldsymbol{\sigma}$ and $\boldsymbol{\tau}$ at time t_0 , so that the t dependence is then only parametric.

With the understanding, then, that we are only dealing with parametric t dependences, we can combine (5.74) with the initial condition $U_{t_0,t_0} = \mathbf{1}$ into the integral equation

$$(5.75) \quad U_{t_0,t} = \mathbf{1} - \frac{i}{\hbar} \int_{t_0}^t dt_1 H_{t_1} U_{t_0,t_1},$$

which can be iterated to produce a formal series expansion, a variant of both the Born series of scattering theory and the Dyson series of field theory, of $U_{t_0,t}$ in powers of the (time-integrated) Hamilton operator. It begins with the terms

$$(5.76) \quad U_{t_0,t} = \mathbf{1} - \frac{i}{\hbar} \int_{t_0}^t dt_1 H_{t_1} - \frac{1}{\hbar^2} \int_{t_0}^t dt_1 \int_{t_0}^{t_1} dt_2 H_{t_1} H_{t_2} + \dots$$

For the Hamilton operator (5.62), the Heisenberg equations of motion (5.67) and (5.68) read

$$(5.77) \quad \begin{cases} \frac{d}{dt} \boldsymbol{\sigma}(t) = \boldsymbol{\Omega}_1(t) \times \boldsymbol{\sigma}(t) - \omega(t) \boldsymbol{\sigma}(t) \times \boldsymbol{\tau}(t), \\ \frac{d}{dt} \boldsymbol{\tau}(t) = \boldsymbol{\Omega}_2(t) \times \boldsymbol{\tau}(t) + \omega(t) \boldsymbol{\sigma}(t) \times \boldsymbol{\tau}(t). \end{cases}$$

EXAMPLE 5.1. Let us give the solution of (5.74) for the case when $\boldsymbol{\Omega}_1(t) = 0$, $\boldsymbol{\Omega}_2(t) = 0$:

$$(5.78) \quad \begin{cases} \boldsymbol{\sigma}(t) = \frac{1}{2} [\boldsymbol{\sigma}(t_0) + \boldsymbol{\tau}(t_0)] + \frac{1}{2} [\boldsymbol{\sigma}(t_0) - \boldsymbol{\tau}(t_0)] \cos \varphi - \frac{1}{2} \boldsymbol{\sigma}(t_0) \times \boldsymbol{\tau}(t_0) \sin \varphi, \\ \boldsymbol{\tau}(t) = \frac{1}{2} [\boldsymbol{\sigma}(t_0) + \boldsymbol{\tau}(t_0)] - \frac{1}{2} [\boldsymbol{\sigma}(t_0) - \boldsymbol{\tau}(t_0)] \cos \varphi + \frac{1}{2} \boldsymbol{\sigma}(t_0) \times \boldsymbol{\tau}(t_0) \sin \varphi, \end{cases}$$

where

$$(5.79) \quad \varphi = 2 \int_{t_0}^t dt' \omega(t').$$

One can verify by inspection that (5.78) solves (5.77). \square

Summarizing the above discussions, we have established the following.

THEOREM 5.7. *Let (5.11) and (5.12) be satisfied. Then we have*

$$(5.80) \quad \begin{cases} \frac{d}{dt}\boldsymbol{\sigma}(t) = \frac{1}{i\hbar}[\boldsymbol{\sigma}, H](t) = \boldsymbol{\Omega}_1(t) \times \boldsymbol{\sigma}(t) - \omega(t)\boldsymbol{\sigma}(t) \times \boldsymbol{\tau}(t), \\ \frac{d}{dt}\boldsymbol{\tau}(t) = \frac{1}{i\hbar}[\boldsymbol{\tau}, H](t) = \boldsymbol{\Omega}_2(t) \times \boldsymbol{\tau}(t) + \omega(t)\boldsymbol{\sigma}(t) \times \boldsymbol{\tau}(t) \end{cases}$$

and

$$(5.81) \quad \begin{cases} \boldsymbol{\sigma}(t) = U_{t,t_0}\boldsymbol{\sigma}(t_0)U_{t_0,t} \\ \boldsymbol{\tau}(t) = U_{t,t_0}\boldsymbol{\tau}(t_0)U_{t_0,t} \end{cases}, \quad \text{for any } t_0, t \geq 0.$$

\square

6. Conclusion

New or improved versions of the elementary devices cited in this paper are constantly emerging. For example, in the design of cavity QED, instead of using a particle beam to shoot atoms through an optical cavity as illustrated in Fig. 3.2, there have been proposals to enclose ion traps inside a cavity. Thus, such proposals incorporate both features of ion traps and cavity QED as studied in this paper. Even though it is not possible for us to describe *all* major types of contemporary quantum computing devices or proposals, we hope that our mathematical analysis and derivations herein have provided reasonably satisfactory rigor and basic principles useful in helping future interdisciplinary research in quantum computation.

From the control-theoretic point of view, the best theoretical model for laser and quantum control seems to be the Schrödinger equation offered by (5.11) with the Hamiltonian given by (5.4), wherein the $\boldsymbol{B}_j(t)$'s and $J_{jk}(t)$'s are the *bilinear controllers*. Equivalently, the Heisenberg's equations of motion as presented in Theorem 5.7 (which deal with only two quantum dots) form a *bi-trilinear control system* with $\boldsymbol{\Omega}_1(t)$ and $\boldsymbol{\Omega}_2(t)$ therein as bilinear controllers, while $\omega(t)$ is a *trilinear controller*. Such control systems (as presented in Theorem 5.7, e.g.) look nearly identical to the classical rigid body rotation dynamics and, thus, a fair portion of the existing control results appear to be readily applicable. In our discussion in Section 5, we have derived certain formulas for the shaping of laser pulses (see (5.34), (5.44), (5.45), (5.53), etc.) which can achieve the desired elementary 1-bit and 2-bit elementary quantum gates. However, we wish to emphasize that such laser pulse shaping is *underutilized* as far as the control effects are concerned. To obtain more optimal control effects, *feedback strategies* need to be evaluated. Quantum feedback control is currently an important topic in quantum science and technology.

For the models of 2-level atoms, cavity QED and ion traps, our discussions here have shown that the admissible class of controllers is quite limited, the reason being that the control or excitation laser must operate at specified frequencies in order to stay within the two or three levels, and to avoid the excitation of unmodeled dynamics. We can exercise control mainly through the duration of the activation of laser pulses, such as (3.20) has shown.

There are many interesting mathematical problems in the study of laser-driven control systems. Quantum computing/computer contains an abundant source of such problems for mathematicians and control theorists to explore.

References

- [1] N.W. Ashcroft and N.D. Mermin, *Solid State Physics*, Chap. 32, Saunders, Philadelphia, 1976.
- [2] A. Barenco, A universal two bit gate for quantum computation, *Proc. Royal Soc. London A*, **449** (1995), 679–693.
- [3] A. Barenco, C. H. Bennett, R. Cleve, D. P. DiVincenzo, N. Margolus, P. Shor, T. Sleator, J. A. Smolin and H. Weinfurter, Elementary gates for quantum computation, *Phys. Rev. A*, **52** (1995), 3457–3467.
- [4] J-L Brylinski and R. Brylinski, Universal Quantum Gates, in *Mathematics of Quantum Computation*, R. Brylinski and G. Chen, eds., Chapman & Hall/CRC, Boca Raton, Florida, 2002, 101–116.
- [5] G. Burkard, D. Loss and D. P. DiVincenzo, *Phys. Rev. B* **59** (1999), 2070.
- [6] G. Burkard, H.-A. Engel and D. Loss, Spintronics, quantum computing and quantum communications in quantum dots, in *Fundamentals of Quantum Information*, W. Dieter Heiss, ed., Springer-Verlag, Berlin and Heidelberg, 2002, 241–265.
- [7] J. I. Cirac and P. Zoller, *Phys. Rev. Lett.* **74** (1995), 409.
- [8] D. Deutsch, Quantum computational networks, *Proc. Royal Soc. London A*, **425** (1989), 73–90.
- [9] D. Deutsch, A. Barenco and A. Ekert, Universality in quantum computation, *Proc. Royal Soc. London A*, **449** (1995), 669–677.
- [10] Z. Diao, M. S. Zubairy and G. Chen, A quantum circuit design for Grover’s algorithm, *Zeit. für Naturforsch.* **56a** (2001), 879–888.
- [11] P. A. M. Dirac, *The Principles of Quantum Mechanics*, 4th edition, (Clarendon Press, Oxford, 1958).
- [12] D. P. DiVincenzo, Two-bit quantum gates are universal for quantum computation, *Phys. Rev. A*, **51** (1995), 1015–1022.
- [13] H.-A. Engel and D. Loss, *Phys. Rev. Lett.* **86**, 4648 (2001).
- [14] R.J. Hughes et al., The Los Alamos trapped ion quantum computer experiment, *Fortsch. Phys.* **46** (1998), 329–362.
- [15] D. Jonathan and M.B. Plenio, *Phys. Rev. Lett.* **87** (2001), 127901.
- [16] S. Lloyd, Almost any quantum logic gate is universal, *Phys. Rev. Lett.* **75** (1995), 346–349.
- [17] S. Lomonaco, A Rosseta stone for quantum mechanics with an introduction to quantum computation, quant-ph/0007045, July 2000.
- [18] D. Loss and D.P. DiVincenzo, *Phys. Rev. A* **57**, 120 (1998).
- [19] C. Monroe, D. M. Meekhof, B. E. King, W. M. Itano and D. J. Wineland, *Phys. Rev. Lett.* **82** (1999), 1971.
- [20] M. A. Nielsen and I. L. Chuang, *Quantum Computation and Quantum Information*, Cambridge University Press, Cambridge, U.K., 2001.
- [21] A. Rauschenbeutel, G. Nogues, S. Osnaghi, P. Bertet, M. Brune, J. M. Raimond and S. Haroche, *Phys. Rev. Lett.* **83** (1999), 5155.
- [22] C. A. Sackett et al., Experimental entanglement of four particles, *Nature* **404** (2002), 256.
- [23] J. Schliemann and D. Loss, Entanglement and quantum gate operations with spin-qubits in quantum dots, cond-mat/0110150, Oct. 2001, to appear in “Future Trends in Microelectronics: The Nano Millenium”, S. Luryi, J. Xu and A. Zaslavsky, ed., Wiley, New York.
- [24] J. Schwinger, *Quantum Mechanics. Symbolism of Atomic Measurements*, ed. by B.-G. Englert (Springer-Verlag, Berlin and Heidelberg, 2001)
- [25] M. O. Scully and M. S. Zubairy, *Quantum Optics*, Cambridge Univ. Press, Cambridge, U.K., 1997.
- [26] A. Sørensen and K. Mølmer, *Phys. Rev. Lett.* **82** (1999), 1971.

- [27] Special Issue on Experimental Proposals for Quantum Computation, *Fortschr. Phys.* **48** (2000), 9–11.
- [28] D. J. Wineland, C. Monroe, W. M. Itano, D. Liebfried, B. E. King and D. M. Meekhof, *J. Res. Nat. Stand. Tech.* **103** (1998), 259–328.

DEPARTMENT OF MATHEMATICS, TEXAS A&M UNIVERSITY, COLLEGE STATION, TX 77843,
U.S.A.

E-mail address: `gchen@math.tamu.edu`

DEPARTMENT OF PHYSICS, TEXAS A&M UNIVERSITY, COLLEGE STATION, TX 77843, U.S.A.

E-mail address: `church@physics.tamu.edu`

DEPARTMENT OF PHYSICS, NATIONAL UNIVERSITY OF SINGAPORE, SINGAPORE

E-mail address: `phyebg@nus.edu.sg`

DEPARTMENT OF PHYSICS, TEXAS A&M UNIVERSITY, COLLEGE STATION, TX 77843, U.S.A.

E-mail address: `zubairy@physics.tamu.edu`